MEDWIN PUBLISHERS
Committed to create value for Researchers

Petroleum & Petrochemical Engineering Journal
ISSN: 2578-4846

Modelling and Simulation of Riser Reactor of a Commercial Fluid Catalytic Cracking Unit Using 6-Lump Kinetics of Vacuum Gas Oil

Olafadehan OA[1]*, Daramola OM[1], Sunmola OP[1] and Abatan GO[2]

[1]Department of Chemical and Petroleum Engineering, University of Lagos, Akoka-Yaba, Lagos 101017, Nigeria

[2]Department of Chemical Engineering, Covenant University, Canaan Land, Ota, Ogun State, Nigeria

Research article

Volume 3 Issue 3

Received Date: June 12, 2019

Published Date: July 12, 2019

DOI: 10.23880/ppej-16000194

***Corresponding author:** Olaosebikan Abidoye Olafadehan, Department of Chemical and Petroleum Engineering, University of Lagos, Akoka-Yaba, Lagos 101017, Nigeria, Email: oolafadehan@unilag.edu.ng/ olafadehan@yahoo.com

Abstract

This work presents a one-dimensional adiabatic mathematical model for the riser reactor of a commercial fluid catalytic cracking unit, FCCU. The cracking reactions in the riser reactor were based on six-lump kinetics of the catalytic cracking of vacuum gas oil, taking cognizance of diffusion resistance, which is a departure from the general norm in the literature. Moreover, two-phase hydrodynamic model for the riser reactor, coke-on-catalyst deactivation model as well as heat transfer resistance between the fluid and solid phases were considered. Two vaporization approaches (the instantaneous and one-dimensional vaporization) of the feedstock were investigated. The developed model was a set of eleven highly non-linear, coupled and stiff ordinary differential equations, ODEs, which was numerically solved with an implicit MATLAB built-in solver, ode23tb, designed deliberately for handling stiff differential equations to circumvent the problem of instability associated with explicit methods. The industrial plant data of China National Petroleum Corporation (CNPC) were used to validate the simulated results of this study. Moreover, our simulated results revealed that the mode of vaporization of the feedstock had influence on the conversion, yield and other process parameters at the riser reactor outlet. Excellent agreements were achieved between the CNPC FCCU plant data and the simulated results of this study for instantaneous vaporization of feedstock, with AAD being $< \pm 5\%$ in all cases investigated, where the optimal yields of the cracked products needed to meet market demands and ensuring maximum profit were achieved

Keywords: Adiabatic; FCCU riser reactor; Catalytic cracking; Six-lump; Diffusion resistance; Ode23tb

Introduction

The fluid catalytic cracking unit, FCCU, is the heart or workhorse of a modern refinery. Higher profitability of a refinery is synonymous with FCCU. That is why nearly every major fuels refinery, including China National Petroleum Corporation, CNPC, in the Republic of China, has an FCCU. The FCCU is one of the most significant and sophisticated contributions to petroleum refining technology. Its capacity is usually one-third of atmospheric crude distillation capacity. Generally, FCCU contributes the highest volume (35 vol %) to the gasoline pool through the catalytic conversion of heavy oil feedstock in the riser reactor, with the Reformer, Alkylation and Isomerization contributing 30, 20 and 15 vol % respectively. Consequently, oil refineries use fluid catalytic cracking to correct the imbalance between the market demand for gasoline and the excess of heavy, high boiling range products resulting from the distillation of crude oil. The fluid catalytic cracking plant ensures the conversion of heavy oil feedstock into a high octane number gasoline and other valuable products such as olefin which serves as the feedstock in the petrochemical industry. Typically, the FCCU is an arrangement of important item of equipment of riser reactor-disengager-regenerator, as shown in Figure 1 for the Catalyst Plant of China National Petroleum Corporation (CNPC), which is under investigation in this study.

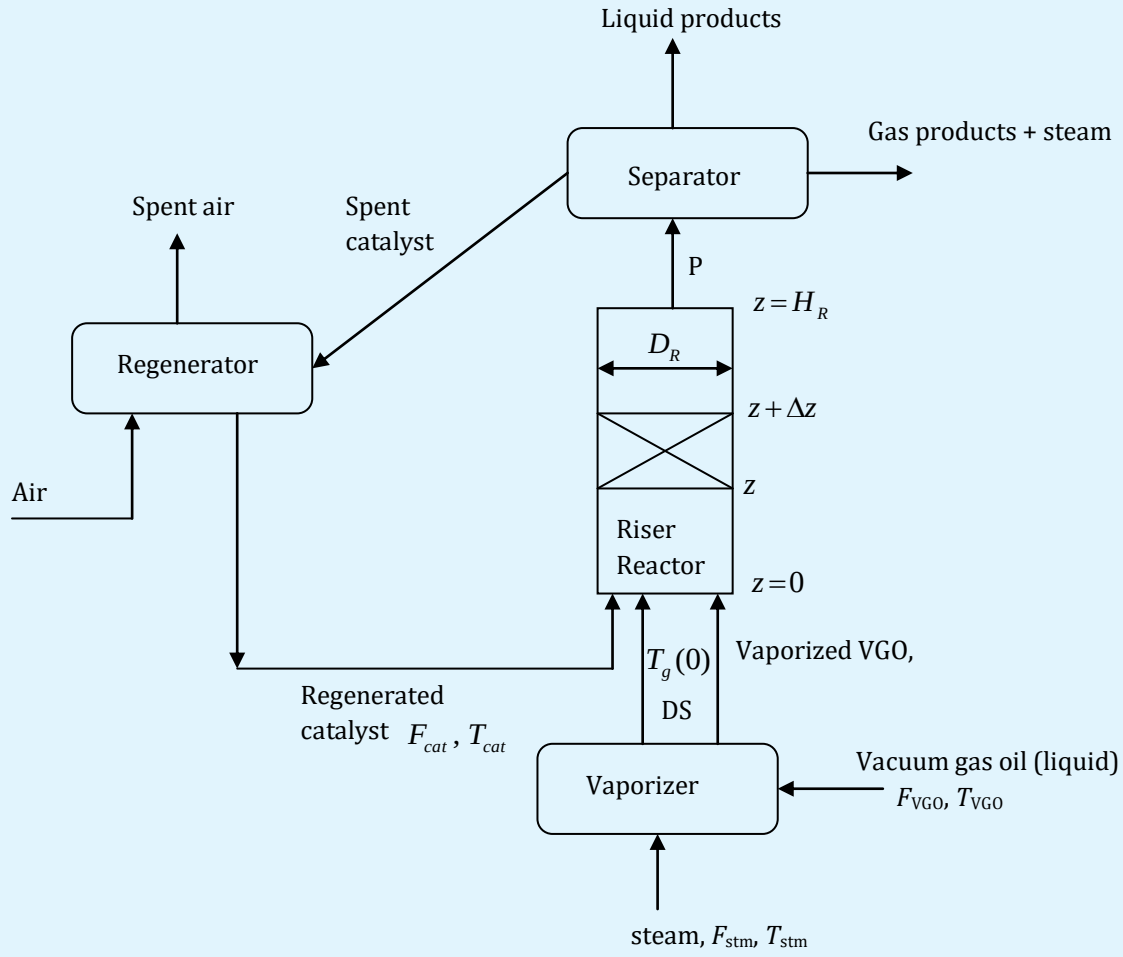

Figure 1: Block diagram of the reactor-regeneration section of a typical FCCU: DS represents dispersion steam, P represents steam +spent catalyst+cracked products from the riser reactor.

Copyright© Olafadehan OA, et al.

The feedstock was a residue of FCCU of CNPC, whose properties are presented in Table 1 [1].

Parameter	Value	Parameter	Value
Density at 20°C	0.919 g/cm³	**SARA composition**	
Viscosity at 100°C	14.15 mm²/s	Saturates	57.8
Molecular weight	444 kg/kmol	Aromatics	35.5
Basic nitrogen	689 ppm	Resin and asphaltenes	6.7
CCR	4.13 wt%	**Simulated distillation**	
Elemental composition		Initial Boiling Point (IBP)	261°C
Carbon	86.81 wt %	10%	356°C
Hydrogen	12.22 wt%	30%	415°C
Sulphur	0.61 wt%	50%	461°C
Nitrogen	0.30 wt%	70%	528°C
		90%	644°C

Table 1: CNPC FCCU feedstock properties [1].

The in-situ crystallized FCC catalyst was developed by Lanzhou Petrochemical Research Centre of CNPC and produced by Catalyst Plant of CNPC Lanzhou Petrochemical Corporation. The main properties of the catalyst are presented in Table 2 [1].

Parameter	Value	Parameter	Value
Pore volume	0.37 cm³/g	Attrition index	1.0 wt%
Surface area	338.8 m²/g	Particle size distribution	
Rare earths	6.77 wt%	0-40 μm	6.05 wt%
Microactivity index	60	40-80 μm	28.25 wt%
Packing density	0.87 g/cm³	> 80 μm	65.70 wt%

Table 2: Properties of catalyst produced by Catalyst Plant of CNPC [1].

The unit is all continuous process that operates 24 h a day for as long as 3-5 years between scheduled shutdowns for routine maintenance. Its main products are highlighted in Figure 2.

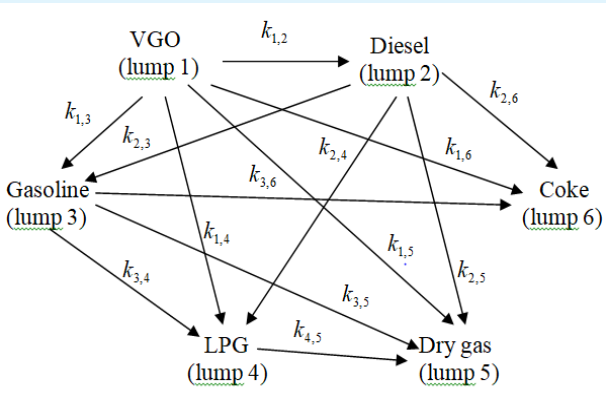

Figure 2: Six-lump model of vacuum gas oil catalytic cracking in the riser reactor [2].

Almost all the endothermic catalytic cracking of the vacuum gas oil, and coke deposition on the catalyst occur in the riser reactor, while in the regenerator reactor, air is used to burn off the spent coke for catalyst regeneration [3,4]. The riser reactor is probably the most focused item of equipment in an FCCU. Its modeling is very complicated for reasons of many complex reactions occurring in it, coupled with mass and heat transfer resistances between the gas and solid phases, and catalyst deactivation kinetics. Hence, a detailed mathematical model of the riser reactor should include all the significant physical phenomena and detailed reaction and deactivation kinetics [5], as was done in these studies. However, this poses a challenge in modelling FCCU riser reactor. For simplification, the kinetic mechanism of the fluid catalytic cracking was investigated in the literature by dividing the feed and products into components commonly known as "lump", as shown in Figure 2. The first kinetic model for the catalytic cracking of heavy oil, developed by Weekman [6], was based on three lumps: feedstock lump, gasoline lump, and dry gas+coke lump. The model may be applied to any type of feedstock, only that it may not capture the

Copyright© Olafadehan OA, et al.

prediction of the yields of other valuable products such as liquefied petroleum gas (LPG), light cycle oil (LCO) and so on. Weekman and Nace [7] proposed a kinetic model of three lumps: stock oil, gasoline, and C_3+C_4+dry gas+coke, to account for stock oil (gas oil) conversion and gasoline yield in isothermal fixed, moving and fluid bed reactors, without considering mass and heat transfer effects. Moreover, the model was only capable of predicting the gasoline yield but failed to consider the effects of the coke deposited on the catalyst surface. Coke is mainly the by-product of the cracking reactions and it provides the heat required for the endothermic reactions. Without considering the effect of the coke, the conversion is not appropriate. Starting from these models, and with the increasing power of computation and knowledge on the mechanism of the catalytic cracking reactions of heavy oil in the riser reactor, more complex kinetic models for catalytic cracking of heavy oil were developed in order to have a more detailed description of the compositional behaviour of FCCU riser reactors, without the incorporation of diffusion resistance. These models were based on 4-lump [8-12], 5-lump [13-15), 6-lump [16,17], 7-lump [18-20], 8-lump [21,22], 10-lump [23], 11-lump [24,25], 12-lump [26] and 19-lump [27], without taking cognisance of diffusion resistance, except the work of Olafadehan, et al. (2018) [20]. A comprehensive review was presented by Pinheiro, et al. [28] on the subject of fluid catalytic cracking process modelling, simulation and control. Obviously, the number of lumps of the proposed kinetic models for catalytic cracking of heavy oil may be increased to obtain more detailed descriptions of the catalytic cracking reactions and product distribution [29,30]. This increases the number of kinetic parameters that need to be experimentally obtained and hence the resulting model equations becoming complicated. So, as a compromise, one may be constrained to choose a less number of lumps that can still provide useful information on the yields of marketable products. Which informed the use of the six-lump kinetics for the vacuum gas oil conversion in the riser reactor in our study, with the incorporation of diffusion resistances, which are sparingly investigated kinetically in the literature.

Many of the mathematical models in the literature describe the riser reactor with one-dimensional mass, energy and chemical species balances [31-34]. Alexiadis, et al. [15] investigated the catalytic cracking of pure n-decane (which represented the conventional gas oil feed) and admixture of n-decane with 10 wt% 2-ethylphenol, EP (which served as a model component for Hydro Deoxygenated (HDO) bio-oil over a series of 12 Faujasite zeolites in a fluid catalytic cracking unit. In their work, they did observe that EP induced fast deactivation of the Faujasites, which was more pronounced over materials with low mesoporous surface area and/or volume. Moreover, the increase in gasoline selectivity and decrease in LPG selectivity with time-on-stream (TOS) were more pronounced for an EP-containing feeds. John, et al. [17] considered detailed steady state model of an industrial FCCU in Sudan, with a newly proposed six-lump kinetic model that cracks gas oil into diesel, gasoline, LPG, dry gas and coke. In their work, frequency factors, activation energies and heats of reaction for the kinetics of catalytic cracking and model parameters were estimated using an optimization technique in gPROMS software to minimize the sum of squared errors between experimental and calculated values. The major industrial riser reactor weight fractions of diesel and gasoline were predicted to be 0.1842 and 0.4863 with % errors of 0.81 and 2.71 respectively when compared with the plant data. In our study, comprehensive and feasible one-dimensional models were employed to a commercial CNPC-FCCU riser reactor using six-lump kinetics of catalytic cracking of vacuum gas oil, with the incorporation of mass and heat transfer resistances, which is a deviation from the general norm in the literature. Normally, for industrial applications, the main goal of FCCU-riser reactor simulations is to predict accurately, for a particular set of operating conditions, the mass fraction of each component (diesel, gasoline, LPG, dry gas, and so on) at the riser reactor outlet, so that the set of input parameters may be changed, aiming to increase (or maximize) the conversion of a specific product. Our developed mathematical models of the riser-type of this FCCU contained the following components: kinetic model of the catalytic cracking of vacuum gas oil, catalyst deactivation model, hydrodynamic model of the riser reactor, material, force and energy balances. A computational code was written in MATLAB environment to proffer numerical solution of the resulting system of model equations. The simulated results were validated by comparison with industrial plant data of the vacuum gas oil conversion and yield. Our attempt in modelling and simulation of an industrial FCCU-riser reactor data is sufficiently precise to be used for the design of new units and for system control and optimization of operating conditions of any FCCU-riser reactor for the reason of demonstration of our model to be used as a powerful and simple tool for design, control and optimization of FCCUs, combining accuracy with less computational time of about 5 s to obtain accurate numerical solutions when simulating actual FCCU riser reactor operation.

Copyright© Olafadehan OA, et al.

Development of Mathematical Models for Riser Reactor of Commercial Fluid Catalytic Cracking Unit

The Mathematical Models

The control-relevant dynamics of the riser reactor-regenerator section of a typical commercial FCCU can be described by modelling the plant as four subsystems, as shown in Figure 1. In Figure 1, the oil feed and steam, having passed through the vaporizer, enter the catalytic riser together with the regenerated catalyst, where cracking of vacuum gas oil into lighter products starts as it contacts the hot regenerated catalyst from the regenerator. The catalyst is made to rise by steam introduced at the base of the riser between the regenerator and the feed inlet point. The vaporized feed and the catalyst pass through the riser into disengager for cracked products and catalyst separation. After which, the spent catalyst flows down by gravity into the regenerator, where air is used to burn off the coke deposited on the catalyst in order to return it to a stable state for catalyzing the cracking reaction.

Model for the Vaporizer Subsystem

The vacuum gas oil and steam pass through the vaporizer, as shown in Figure 1. Hence, by a consideration of the energy balance for the fluid streams (VGO and dispersion steam) entering the riser reactor at $z=0$, Olafadehan et al. (2018) presented the inlet temperature of the vapour phase, $T_{g,in}$, to the riser reactor thus:

$$T_{g,in}=T_g(0)=\frac{F_{VGO}\left[c^L_{p,VGO}\left(T_{VGO}-T_{vap}\right)+c^V_{p,VGO}T_{vap}-\Delta H_{vap}\right]+F_{stm}c_{p,stm}T_{stm}}{F_{VGO}c^V_{p,VGO}+F_{stm}c_{p,stm}} \quad (1)$$

Mathematical Modelling of the Riser Reactor of FCCU

The mathematical model of the riser-type FCCU contains the following components: kinetic model of the catalytic cracking of vacuum gas oil, deactivation catalyst model, hydrodynamic model of the riser reactor, material balance, force, and energy balances.

Kinetics of Catalytic Cracking of Vacuum Gas Oil in the FCCU-Riser Reactor: The six-lump kinetic model for catalytic cracking of vacuum gas oil as given by Du, et al. [2] is shown in Figure 2. In Figure 2, the feedstock (VGO, n-heptacosane, $C_{27}H_{56}$, b.p. > 350^{o}C) was considered as one lump, which thus represents a simple model that is suitable for a catalytic cracking process using a paraffin atmospheric residue. In Figure 2, diesel (n-hexadecane, $C_{16}H_{34}$, b.p. > 221^{o}C, S.G. at 15^{o}C=0.9350), gasoline (b.p. of 38.5-221^{o}C, S.G. at 15^{o}C=0.7585) and LPG (C_3+C_4, S.G. at 15^{o}C=0.540) and dry gas (H_2+C_1+C_2) were considered individual lump. However, in Figure 2, coke was considered as one lump since it is very important for heat balance of the reaction system.

In the reaction mechanisms of Figure 2 for catalytic cracking of vacuum gas oil, it was assumed that the reactions of converting vacuum gas oil and diesel into light products were irreversible second order while other reactions were irreversible first-order. All reactions take place in the gas phase. Moreover, mass and heat transfer resistances between the reacting fluid and the catalyst were incorporated in the kinetic model, as against previous works in the literature.

The magnitude of the effectiveness factor, η, $(0<\eta<1)$ indicates the relative importance of diffusion and reaction limitations. The internal effectiveness factor of the particle, η, is defined as:

$$\eta=\frac{rate\ of\ \ reaction\ with\ diffusion\ resistance,\ r'_{p,i}}{rate\ of\ \ reaction\ without\ diffusion\ resistance,\ r'_i} \quad (2)$$

$$r'_{p,i}=\eta r'_i \quad (3)$$

The particle effectiveness factor, η, is a direct measure of the extent to which diffusion resistance reduces the rate of chemical reactions in heterogeneous catalysis and it is a function of Thiele modulus. Thiele modulus, φ, is a measure of the ratio of intrinsic reaction rate to diffusion rate and as such equation (3) provides a yardstick for determining the rate determining step in heterogeneous catalysis. The Thiele modulus, φ_n, for an nth-order reaction in a spherical pellet is given by Smith [35]:

$$\phi_n=R\sqrt{\frac{k''_n S_a \rho_{cat} y_{A0}^{n-1}}{D_e}}=R\sqrt{\frac{k_n y_{A0}^{n-1}}{D_e}} \quad (4)$$

However, the internal effectiveness factor for a first-order reaction in a spherical catalyst pellet is given by Smith, [35]:

Copyright© Olafadehan OA, et al.

$$\eta = \frac{3}{\phi_1^2}\left(\phi_1 \coth\phi_1 - 1\right) \quad (5)$$

A similar expression was assumed for a second-order reaction, except for the change in the Thiele Modulus expression.

For a first-order irreversible reaction, the rate of formation of component *i*, with the incorporation of mass transfer resistance, is obtained as (Olafadehan, et al. [20]):

$$r'_{p,i} = \left(\frac{1}{k_g} + \frac{1}{\eta k_{i,j}}\right)^{-1} y_i \equiv k_0 y_i \quad (6)$$

where an overall rate coefficient, k_0, is defined thus:

$$\frac{1}{k_0} = \frac{1}{k_g} + \frac{1}{\eta k_{i,j}} \quad (7)$$

However, for a second-order irreversible reaction, the rate of formation of component *i*, with the incorporation of mass transfer resistance, is obtained as (Olafadehan, et al. [20]):

$$r'_{p,i} = k_g\left\{\left[1 + \left(\frac{1}{2}\right)\frac{k_g}{\eta k_{i,j} y_i}\right] - \sqrt{\left[1 + \left(\frac{1}{2}\right)\frac{k_g}{\eta k_{i,j} y_i}\right]^2 - 1}\right\} y_i \quad (8)$$

Catalyst Deactivation Model Coupled with Reaction Rates: Empirical correlations have been used to express quantitatively the effect of coking on the rates of reaction. For a rational design, a quantitative formulation of the rate of coke deposition is needed to account for the effect of the coking on the riser reactor behaviour. There are two types of catalyst deactivation functions used to describe FCC catalyst deactivation: time-on-stream based function and coke-on-catalyst based function. The latter was used in this study in order to give an insight into the amount of coke deposited on the catalyst surface. Chen and Cao [36] relation between catalyst deactivation function, $\phi(C_{CK})$, and the amount of coke, C_{CK}, on the catalyst in the riser reactor was used for the catalytic cracking of vacuum gas oil:

$$\phi(C_{CK}) = (1 + \alpha C_{CK})^{-\beta} \quad (9)$$

where

$$C_{CK} = \frac{y_{CK} F_{VGO}}{F_c} \quad (10)$$

The catalyst deactivation (or activity) function, $\phi(C_{CK})$ is the ratio of the rate of reaction on a catalyst that has been used for a time, t_c, $\left[-r'_i(t_c)\right]$, to the rate of reaction on a fresh catalyst $(t_c = 0)$, $\left[-r'_i(t_c = 0)\right]$, when there are no diffusion limitations:

$$\phi(C_{CK}) = \frac{-r'_i(t_c)}{-r'_i(t_c = 0)} \quad (11)$$

$$-r'_i(t_c) = \left[-r'_i(t_c = 0)\right]\phi(C_{CK}) \quad (12)$$

Also, $\phi(N)$ and $\phi(A)$ are functions describing the poisoning effect of basic nitrogen and the adsorption effect of aromatics, resins and asphaltene on the reaction rates respectively, and they are respectively given by (Xiong, et al. [1]:

$$\phi(N) = \frac{1}{1 + (k_N y_N t_c / COR)} \quad (13)$$

$$\phi(A) = \frac{1}{1 + K_A(y_A + y_R + y_{ASP})} \quad (14)$$

Hence, for catalytic cracking of vacuum gas oil, Equations (9), (12-(14) were combined to obtain the rate of disappearance of lump *i*, $\left[-r'_i(t_c)\right]$ as follows:

$$-r'_i(t_c) = \frac{\left[-r'_i(t_c = 0)\right](1 + \alpha C_{CK})^{-\beta}}{\left[1 + (k_N y_N t_c / COR)\right]\left[1 + K_A(y_A + y_R + y_{ASP})\right]} \quad (15)$$

Hydrodynamic Model of the Riser Reactor: The hydrodynamics presented herein tries to mimic the real situation in a riser reactor. The detailed hydrodynamic model of the riser reactor employed in this study can be found in Olafadehan, et al. [20], and summarized thus:

Copyright© Olafadehan OA, et al.

$$\Psi=\frac{v_g}{v_c}=\frac{U_g}{\in_g v_c}=1+5.6Fr^{-1}+0.47Fr_t^{0.41};$$

$$U_g=\frac{F_g}{\rho_g A_R};\ v_g=\frac{F_g}{\rho_g A_R \in_g};\ Fr=\left(U_g\right)_0/\sqrt{gD_R};$$

$$Fr_t=U_t/\sqrt{gD_R};\ Ar=\rho_g\left(\rho_c-\rho_g\right)gD_p^3/\mu_g^2;$$

$$\mathrm{Re}_t=\frac{Ar}{18+\left(2.3348-1.7439\Phi\right)Ar^{0.5}};$$

$$U_t=\mathrm{Re}_t\,\mu_g/\left(\rho_g D_p\right);\ \rho_g=\frac{p\overline{M}_g}{1000R_uT_g};$$

$$F_g=F_f\left(y_{VGO}+y_{LCO}+y_{GA}+y_{LG}\right)+F_{stm};\ \in_g=1-\in_c;$$

$$\overline{M}_g=\frac{1}{y_{VGO}/M_{VGO}+y_{LCO}/M_{LCO}+y_{GA}/M_{GA}+y_{LG}/M_{LG}+F_{stm}/18F_f};$$

$$\in_c=\frac{F_c}{\rho_c v_c A_R};$$

$$\rho_c=\left(1-\varepsilon_c\right)\rho_p;\ \in_g=\frac{U_g\rho_c}{U_g\rho_c+\Psi G_c}$$

where Ψ is slip factor; v_g is interstitial gas velocity in the riser; U_g is superficial gas velocity in the riser reactor; $\in_c$ is volume fraction of the cluster phase (catalyst+coke); $\in_g$ is volume fraction of the gas phase (VGO+steam); Fr is dimensionless Froude number; Fr_t is dimensionless Froude number based on terminal velocity; ρ_g is density of gas phase (heavy oil+steam) in the riser; ρ_c is density of cluster phase (catalyst+coke) in the riser; A_R is cross-sectional area of riser; g is acceleration due to gravity; Ar is Archimedes number; Re_t is Reynolds number based on terminal velocity; U_t is particle terminal velocity; p is riser pressure in the riser; y_i is yield of lump i; $\overline{M}_g$ is average vapour phase molecular weight; R_u is universal gas constant; T_g is temperature of fluid phase in the riser; G_c is mass flux of cluster phase (catalyst+coke) in the riser; ε_c is average voidage of the clusters; ε_g is average voidage of the gas phase; and M_i is the molecular weight of lump *i*.

The catalyst residence time, t_c, was calculated using the expression:

$$\frac{dt_c}{d\sigma}=\frac{H_R A_R \rho_{cat}\Psi}{F_{cat}\Psi+F_g\left(1-y_{CK}\right)\rho_{cat}RT_g/p\overline{M}_g} \quad (16)$$

while the residence time, t_g, of the gas phase was calculated thus:

$$t_g=z/v_g=H_R\sigma\in_g/U_g \quad (17)$$

The cluster phase velocity, v_c, in the riser reactor was determined by the momentum equation of Tsuo and Gidaspow [37], and summarized by Gupta, et al.[5], Fernandes, et al. [38] and Han and Chung [34], which is given in dimensionless form thus:

$$\frac{d\bar{v}_c}{d\sigma}=\frac{H_R}{\left(v_c\right)_0}\left\{\frac{C_f\left[v_g-\bar{v}_c\left(v_c\right)_0\right]A_R}{F_c}-\frac{2f_c\bar{v}_c\left(v_c\right)_0}{D_R}-\frac{g}{\bar{v}_c\left(v_c\right)_0}\right\} \quad (18)$$

where

$$C_f=0.5\rho_g C_D A_p\left|v_g-\bar{v}_c\left(v_c\right)_0\right| \quad (19)$$

$$C_D=\begin{cases}\dfrac{24}{\mathrm{Re}}\left(1+0.15\,\mathrm{Re}^{0.687}\right) & for\ \mathrm{Re}<1000\\ 0.44 & for\ \mathrm{Re}\geq 1000\end{cases} \quad (20)$$

$$\mathrm{Re}=\frac{\rho_g\varepsilon_g\left|v_g-\bar{v}_c\left(v_c\right)_0\right|D_c}{\mu_g} \quad (21)$$

$$A_p=1.5\varepsilon_c/D_c \quad (22)$$

For catalytic cracking of vacuum gas oil, the viscosity of the gas phase, μ_g, was calculated according to Bromley and Wilke [39] thus:

$$\mu_g=\sum_{i=VGO,D,GA,LPG,DG,stm}\left(\frac{y_i\mu_i}{y_i+\sum_{\substack{i=VGO,D,GA,LPG,DG,stm\\ j\neq i}}\Omega_{ij}y_j}\right) \quad (23)$$

Copyright© Olafadehan OA, et al.

where

$$y_i = F_i / F_g \quad i = VGO, D, GA, LPG, DG, stm \quad (24)$$

$$\Omega_{ij} = \frac{\left[1+\left(\mu_j/\mu_i\right)^{0.5}\left(M_j/\overline{M}_g\right)^{0.25}\right]^2}{\sqrt{8\left(1+M_i/M_j\right)}} \quad (25)$$

In the above equations, the gas phase viscosity of the i^{th} component, μ_i, was calculated by the following correlation (American Petroleum Institute [40]):

$$\mu_i = 18.9943 + 0.061819\theta + 0.017352 M_i + 9.08118\times10^{-6}\theta M_i - 1.00638\times10^{-5}\theta^2 - 1.04832\times10^{-4} M_i^2$$

$$-0.136695\,\theta/M_i - 3.20527\,In\,M_i - 8.35025\times10^{-3}\theta\,In\,M_i \quad (26)$$

where θ is temperature in ^oC.

The viscosity of steam, μ_{stm}, was determined by the correlation of Daubert and Danner [41]:

$$\mu_{stm} = \frac{7.6190\times10^{-8}T^{0.92758}}{1+211.6/T-4670/T^2} \quad (27)$$

where T is temperature in K.

Continuity Equation of Component in FCCU-Riser Reactor: The component mass balance taken over an elemental volume of the riser reactor, shown in Figure 1, for each of the lumps was obtained as follows:

$$\left(\frac{\partial \rho y_i}{\partial t}\right)_z + \frac{F_g}{A_R}\left(\frac{\partial y_i}{\partial z}\right)_t = \rho_g \in_g r'_{p,i},\ i = VGO, D, GA, LPG, DG, CK \quad (28)$$

VGO, D, GA, LPG, DG and CK represent vacuum gas oil, diesel, gasoline, liquefied petroleum gas, dry gas and coke respectively. The assumptions inherent in the model are: (1) Adiabatic and one-dimensional transported ideal plug flow for gas (VGO+steam) and cluster phase (catalyst+coke) but with different velocities, no axial back-mixing and no radial dispersion; (2) Diffusion resistances are significant, and no adsorption within the catalyst particle; (3) There is no heat loss from the riser reactor; (4) The pressure drop along the riser length is due to the hydrostatic head of catalyst, solid acceleration, solid and gas friction in the riser reactor (Pugsley and Berruti [42,43]; (5) A variable gaseous superficial velocity with axial position along the riser length is assumed; (6) The catalyst particles are assumed to move as clusters to account for the observed high slip velocities; (7) The coke exists as solid and its deposition on the catalyst particles does not affect the fluid flow; (8) In each section of riser, the cluster (catalyst and coke) and gas (hydrocarbon vapours) have different temperature in order to account for the heat transfer between the fluid and the solid phases Olafadehan, et al. [20]; (9) The reactor dynamics is fast enough to justify a quasi-steady state model; and (10) Two approaches of the vaporization of the feedstock are considered: (i) Instantaneous and complete vaporization of vacuum gas oil occurred at the reactor entrance; and (ii) One-dimensional vaporization of the VGO.

At steady state, in dimensionless form, for catalytic cracking of vacuum gas oil in the riser reactor, Equation (28) becomes:

$$\frac{S_v \rho_{cat}}{\rho_g \in_g^2}\left(\frac{dy_i}{d\sigma}\right) = r'_{p,i}, \qquad i = VGO, D, GA, LPG, DG, CK \quad (29)$$

where

$$G_v = \frac{F_g}{A_R} = \frac{S_v H_R \rho_c}{\in_g} \quad (30)$$

Writing the rate of formation, $r'_{p,i}$, for lump i in the reaction network of Figure 2, the resulting dimensionless steady-state model for the yield of each lump in the riser reactor of CNPC-FCCU was obtained from Equation (29) thus:

$$\frac{dy_{VGO}}{d\sigma} = -\frac{\left(k_{1,2}+k_{1,3}+k_{1,4}+k_{1,5}+k_{1,6}\right)(COR)\rho_g \in_g^2 y_{VGO}^2}{S_v\rho_{cat}\left[1+\left(k_N y_N t_c/COR\right)\right]\left[1+K_A\left(y_A+y_R+y_{ASP}\right)\right]}\left(1+\frac{\alpha y_{CK} F_{VGO}}{F_c}\right)^{-\beta} \quad (31)$$

$$\frac{dy_D}{d\sigma} = \frac{\rho_g \in_g^2 (COR)\left[\alpha_{1,2}k_{1,2}y_{VGO}^2 - \left(k_{2,3}+k_{2,4}+k_{2,5}+k_{2,6}\right)y_D^2\right]}{S_v\rho_{cat}\left[1+\left(k_N y_N t_c/COR\right)\right]\left[1+K_A\left(y_A+y_R+y_{ASP}\right)\right]}\left(1+\frac{\alpha y_{CK} F_{VGO}}{F_c}\right)^{-\beta} \quad (32)$$

Copyright© Olafadehan OA, et al.

$$\frac{dy_{GA}}{dt}=\frac{\rho_g \in_g^2 (COR)\left[\alpha_{1,3}k_{1,3}y_{VGO}^2+\alpha_{2,3}k_{2,3}y_D^2-\left(k_{3,4}+k_{3,5}+k_{3,6}\right)y_{GA}\right]}{S_v\rho_{cat}\left[1+\left(k_N y_N t_c/COR\right)\right]\left[1+K_A\left(y_A+y_R+y_{ASP}\right)\right]}\left(1+\frac{\alpha y_{CK}F_{VGO}}{F_c}\right)^{-\beta} \quad (33)$$

$$\frac{dy_{LPG}}{d\sigma}=\frac{\rho_g \in_g^2 (COR)\left(\alpha_{1,4}k_{1,4}y_{VGO}^2+\alpha_{2,4}k_{2,4}y_D^2+\alpha_{3,4}k_{3,4}y_{GA}-k_{4,5}y_{LPG}\right)}{S_v\rho_{cat}\left[1+\left(k_N y_N t_c/COR\right)\right]\left[1+K_A\left(y_A+y_R+y_{ASP}\right)\right]}\left(1+\frac{\alpha y_{CK}F_{VGO}}{F_c}\right)^{-\beta} \quad (34)$$

$$\frac{dy_{DG}}{d\sigma}=\frac{\rho_g \in_g^2 (COR)\left(\alpha_{1,5}k_{1,5}y_{VGO}^2+\alpha_{2,5}k_{2,5}y_D^2+\alpha_{3,5}k_{3,5}y_{GA}+\alpha_{4,5}k_{4,5}y_{LPG}\right)}{S_v\rho_{cat}\left[1+\left(k_N y_N t_c/COR\right)\right]\left[1+K_A\left(y_A+y_R+y_{ASP}\right)\right]}\left(1+\frac{\alpha y_{CK}F_{VGO}}{F_c}\right)^{-\beta} \quad (35)$$

$$\frac{dy_{CK}}{d\sigma}=\frac{\rho_g \in_g^2 (COR)\left(\alpha_{1,6}k_{1,6}y_{VGO}^2+\alpha_{2,6}k_{2,6}y_D^2+\alpha_{3,6}k_{3,6}y_{GA}\right)}{S_v\rho_{cat}\left[1+\left(k_N y_N t_c/COR\right)\right]\left[1+K_A\left(y_A+y_R+y_{ASP}\right)\right]}\left(1+\frac{\alpha y_{CK}F_{VGO}}{F_c}\right)^{-\beta} \quad (36)$$

where $\sigma\left(=z/H_R\right)$ is dimensionless riser length; z is axial position in the reactor; H_R is the height of riser reactor; $\alpha_{i,j}\left(=M_i/M_j\right)$ is the chemical measurement coefficient for the reaction of lump *i* to lump *j*, and $k_{i,j}$ is the specific reaction rate constant for the reaction of lump *i* generating lump *j*, expressed using Arrhenius equation thus:

$$k_{i,j}=\left(k_{i,j}\right)_0\exp\left(-\frac{E_{i,j}}{R_uT_g}\right) \quad (37)$$

Using Equation (37) in Equation (7), we have:

$$k_0=\frac{\eta k_g\left(k_{i,j}\right)_0\exp\left(-E_{i,j}/R_uT_g\right)}{k_g+\eta\left(k_{i,j}\right)_0\exp\left(-E_{i,j}/R_uT_g\right)} \quad (38)$$

Thus, the inherent specific reaction rate constants in Equations (31)-(36) were modified according to Equation (38), noting that the rate expressions for second order reactions were used as given in Equation (8).

Force Balance: The expression for predicting the dimensionless pressure drop, $\bar{p}_R$ along the dimensionless height, σ, of the riser reactor was obtained by Olafadehan, et al. [20] thus:

$$\frac{d\bar{p}_R}{d\sigma}=-\frac{1}{u_0^2\left(\rho_g\right)_0}\left\{H_R\rho_c g\left(1-\in_g\right)+\frac{\rho_c\left(1-\in_g\right)\left[\bar{v}_c\left(v_c\right)_0\right]^2}{2\Delta\sigma}+\frac{2H_R f_c\rho_c\left(1-\in_g\right)\left[\bar{v}_c\left(v_c\right)_0\right]^2}{D_R}+\frac{H_R f_g\rho\in_g U_g^2}{D_R}\right\} \quad (39)$$

where $\bar{p}_R$ is dimensionless pressure in the riser reactor; and $p_{in}\left[=u_0^2\left(\rho_g\right)_0\right]$ is the riser inlet pressure. The expression for solids friction factor, f_s, suggested by Konno and Saito [44] was used in this study since it has the widest applicability, and is given by:

$$f_s=\frac{0.0285\left(gD_R\right)^{0.5}}{\nu_c} \quad (40)$$

The gas friction factor, f_g, is calculated from Blasius [45] friction factor, which is expressed as:

$$f_g=0.316\,\mathrm{Re}^{-0.25} \quad (41)$$

Energy Balance for the FCCU-Riser Reactor: Since the reactor operating condition is adiabatic and the reaction is endothermic, energy is consumed. With the incorporation of heat transfer between the solid and gas phases, at steady state, the energy balance over an elemental volume of the reactor for the fluid phase in dimensionless form is given by Olafadehan, et al. [20]:

$$\left(F_{VGO}c_{p,VGO}+F_{stm}c_{p,stm}\right)\frac{d\bar{T}_g}{d\sigma}=\frac{LA_R}{T_{g,in}}\left[\sum_{i=1}^{N}r'_{p,i}\left(-\Delta H_{rxn}\right)_i\in_g\rho_g+hA_{gs}\left(\bar{T}_cT_{cat}-\bar{T}_gT_{g,in}\right)\right] \quad (42)$$

In dimensionless form, the energy balance for the solid phase is given by:

Copyright© Olafadehan OA, et al.

$$\left(F_{cat}c_{p,cat}+F_{CK}c_{p,CK}\right)\frac{d\bar{T}_c}{d\sigma}=LA_R hA_{gs}\left(\bar{T}_g T_{g,in}-\bar{T}_c T_{cat}\right)/T_{cat} \quad (43)$$

where $c_{p,VGO}=\sum_{i=1}^{n} y_i c_{pi}$, $i=D,GA,LPG,DG,CK$, $\bar{T}_g$ is dimensionless temperature of fluid $\left(=T_g/T_{g,in}\right)$; $\bar{T}_c$ is dimensionless temperature of cluster phase $\left[=T_c/(T_c)_0\right]$; $\left(\Delta H_{rxn}\right)_i$ is heat of reaction of lump *i* generating lump *j*; *h* is gas-particulate heat transfer coefficient; and A_{gs} is specific surface area of the particulate based on unit reactor volume, $\left(=6(1-\epsilon_b)/D_p\right)$. Two vaporization approaches of feedstock were considered thus:

1. Instantaneous vaporization, where the feedstock vaporizes as soon as the catalyst gets in contact with it at the riser inlet. The fluid is thus considered as an ideal gas and the enthalpy balances for the fluid and solid phases are given by Equations (42) and (43) respectively.
2. One-dimensional vaporization of the feedstock, where a distillation curve is employed for the fraction of gas oil vaporized, X_{vap}:

$$X_{vap}=0.0027T-0.1254 \quad (44)$$

which is valid from 319.5 – 689.8 K. The gas oil liquid and gas phases take place together for a certain period in the riser reactor. Therefore, the enthalpy of the mixture, h_f, is computed by:

$$h_f=h_V X_{vap}+(1-X_{vap})h_L \quad (45)$$

By employing the data of Farah (2003), the following correlations were obtained (Negrao and Baldessar [46]):

$$h_V=0.0022608T^2+1.2518T+382.81 \quad (46)$$

$$h_L=0.0015072T^2+1.8602T+32.592 \quad (47)$$

which are valid from 319.5 – 689.8 K.
The fluid phase temperature is evaluated by the enthalpy balance as follows:

$$\frac{dh_g}{d\sigma}=\frac{LA_R}{F_g}\left[\sum_{i=1}^{N} r'_{p,i}\left(-\Delta H_{rxn}\right)_i(1-\epsilon_g)\rho_{cat}+hA_e\left(T_c-T_g\right)\right] \quad (48)$$

which can be used in conjunction with Equation (43) to predict the fluid and solid phases' temperatures for one-dimensional vaporization of the feedstock.

Computational Procedure

The developed model equations consist of a set of 11 coupled, highly non-linear first-order ordinary differential equations (16), (18), (31)-(36), (39), (42)/(44) and (43) whose exact analytic solutions are somewhat impossible so, a powerful, robust numerical method for non-linear differential equations must be used. The initial conditions needed to solve these equations are:

$$y_{VGO}(0)=1,\ y_j(0)=0,\left(j=D,GA,LPG,DG,CK\right),\ \bar{v}_c(0)=1,\ t_c(0)=5,\ \bar{p}_R(0)=1,\bar{T}_g(0)=1,\bar{T}_c(0)=1 \text{ at } \sigma=0.$$

The computer program for the numerical solution of the governing differential equations was written in MATLAB R2017a environment, evoking the built-in function ode23tb, which is a solver for initial value problems for stiff ODEs. This function is based on semi-implicit Runge-Kutta method with step-size adjustment strategy for the numerical solution of the developed differential equations with a view to predicting the yield of each lump, temperature and pressure profiles and other process parameters in the riser of an industrial FCCU during the catalytic cracking of vacuum gas oil. This numerical method is efficient, accurate and stiffly stable so any unenvisaged problem of instability associated with explicit methods is removed. Moreover, an iterative excel worksheet was used to study the effect of any change in operating variables on the riser reactor of CNPC FCCU performance.

Before solving the ordinary differential equations, the required physical parameters of the process must be determined first. The respective molecular weights of vacuum gas oil and diesel are 444.0 and 230.0 kg/kmol [1]. According to the six-lump reaction network, the components of vacuum gas oil include diesel, gasoline, LPG, dry gas and coke. n-heptacosane, $C_{27}H_{56}$, and n-hexadecane, $C_{16}H_{34}$, were used as surrogates of VGO and diesel respectively [2], whose specific heat capacities as functions of temperature obtained from Sinnott and

Copyright© Olafadehan OA, et al.

Towler [47] are presented in Table 3. Moreover, to mimic the reactions and compounds being formed in the riser reactor as closely as possible, and in the face of dearth of information on VGO and diesel characterization, a pseudo-component was chosen to represent VGO and diesel, adopted from the work of Du, et al. [2] since the higher the molecular weight of a lump, the more paraffinic it is, an alkane of similar molecular weight was therefore chosen to represent VGO and diesel lumps individually Olafadehan, et al. [20]. Gasoline consists of several hydrocarbons, as revealed in the mass spectrometric analysis of 1 mol of gasoline. For use in the energy balance equation, the specific heat capacities' constants of the components in gasoline lump were obtained from Sinnott and Towler [47] and ASPEN PLUS/HYSYS 9.0, and presented in Tables 4 & 5.

Component	Molecular weight/kg kmol^{-1}	Mass Fraction	a	b	$c\times10^4$	$d\times10^8$
VGO (n-heptacosane)	444.0	1.0	-21.47	2.568	-14.43	30.8
Diesel (n-hexadecane)	230.0	1.0	-13.07	1.529	-8.537	18.497

Table 3: Constants in specific heat capacities of VGO and diesel [47].

S.No.	Component	Mol.wt (kg kmol^{-1})	Mass Fraction	a	b	$c\times10^4$	$d\times10^8$
1.	Propane	44.097	0.0001	-4.224	0.30626	-1.586	3.2146
2.	isobutane	72.151	0.0122	-9.525	0.50660	-2.729	3.7234
3.	n-butane	58.124	0.0629	9.487	0.33130	-1.108	-0.2822
4.	trans-2-butene	56.108	0.0007	18.417	0.25636	0.70138	0.8989
5.	3-methyl-1-butene	70.135	0.0006	21.742	0.38895	-2.007	4.0105
6.	isopentane	86.178	0.1049	-16.634	0.62928	-3.481	6.8496
7.	n-pentane	72.151	0.0586	-3.626	0.48734	-2.580	5.3047
8.	2-methyl-2-butene	70.135	0.0044	11.803	0.35090	-1.117	-0.5807
9.	3,3-dimethyl-1butene	84.162	0.0049	-12.556	0.54847	-2.915	5.2084
10.	2,3-dimethylbutane	86.178	0.0730	-14.608	0.61504	-3.376	6.8203
11.	2-methylpentane	86.178	0.0273	-10.567	0.61839	-3.573	8.0847
12.	n-hexane	86.178	0.0283	-4.413	0.58197	-3.119	6.4937
13.	methylcyclopentane	84.162	0.0083	-50.108	0.63807	-3.642	8.0135
14.	2,2-dimethylpentane	100.205	0.0076	-50.099	0.89556	-6.360	17.358
15.	n-heptane	100.205	0.0063	-5.146	0.67617	-3.651	7.6677
16.	benzene	78.114	0.0076	-33.917	0.47436	-3.0174	7.1301
17.	2,3-dimethylpentane	100.205	0.0390	-7.046	0.70476	-3.734	7.8335
18.	2,2,4-trimethylpentane	114.232	0.0121	-7.461	0.77791	-4.287	9.1733
19.	2,2-dimethylhexane	114.232	0.0055	-9.215	0.78586	-4.400	9.6966
20.	toluene	92.141	0.0550	-24.355	0.51246	-2.765	4.9111
21.	2,3,4-trimethylpentane	114.232	0.0121	-9.215	0.78586	-4.400	9.6966
22.	2-methylheptane	114.232	0.0155	-89.744	1.2422	11.76	46.180
23.	n-octane	114.232	0.0013	-6.096	0.77121	-4.195	8.8551
24	p-xylene	106.168	0.0957	-25.091	0.60416	-3.374	6.8203
25.	n-propylbenzene	120.195	0.0841	-31.288	0.74860	-4.601	10.810
26	1,3,5-trimethylbenzene	120.195	0.0411	-19.590	0.67240	-3.692	7.6995
27.	1,2,4-trimethylbenzene	120.195	0.0213	-4.668	0.62383	-3.263	6.3765
28.	1-methyl-2-ethylbenzene	134.222	0.0307	-16.446	0.69961	-4.120	9.3282
29.	1,2,4,5-tetramethylbenzene	134.222	0.0133	15.265	0.65188	-2.879	3.2569
30.	n-dodecane	170.340	0.0230	-9.328	1.1489	-6.347	13.590
31.	naphthalene	128.174	0.0045	-68.802	0.84992	-6.506	19.808
32.	1-methylnaphthalene	142.201	0.0023	-64.820	0.93868	-6.942	20.155
*Source: Ground water Management Review, Spring, 1990 p.167 (excluding those hydrocarbons whose weight fractions in the gasoline were zero).							

Table 4: Constants in the specific heat capacities of components in gasoline [47].

Copyright© Olafadehan OA, et al.

S/No.	Component	Mol.wt/kg kmol^{-1}	Mass Fraction	a	b	$c\times10^{3}$	$d\times10^{7}$	$e\times10^{10}$	$f\times10^{22}$
33.	2,4,4-trimethylhexane	128.3	0.0087	64.028	0.1427	2.8395	-6.8591	0	0
34.	3,3,4-trimethylhexane	128.3	0.0281	78.651	0.0783	2.85	-6.93	0	0
35.	2,2,4-trimethylheptane	142.3	0.0105	50.953	0.1669	2.8409	-6.8714	0	0
36.	methylpropylbenzene	120.2	0.0351	192.50	-0.3023	2.8825	-7.24356	0	0
37.	1,2,3,4-tetramethylbenzene	148.2	0.0129	3.52×10^{-8}	0.0361	2.73	-10.1	1.59	8.34

Table 5: Constants in specific heat capacities of other components in gasoline obtained from ASPEN PLUS/ HYSYS 9.0. With $g=1$ for serial numbers 33-37.

Since ASPEN PLUS/HYSYS 9.0 is a very good software to characterize feedstock and/or product by pseudo-components from an assay, it was used to populate the VGO and the other components in gasoline properties. These give specific heat capacities as functions of temperature to be used in the energy balance equation. However, representing a property of a lump with a surrogate single component may have significant deviations on the simulated results when compared with plant data. In this study, this was not the case as revealed that there was excellent agreement between simulated results and the plant data for the case of instantaneous vaporization of feedstock.

From the experimental analyses of Du, et al. [2], LPG lump consisted of propane and butane while dry gas consisted of hydrogen, methane, and ethane, whose properties are given in Table 6.

Component	Mol.wt/kg kmol^{-1}	Mass Fraction	a	b	$c\times10^{4}$	$d\times10^{8}$
LPG						
Propane	44.097	0.44	-4.224	0.30626	-1.586	3.2146
n-butane	58.124	0.56	9.487	0.3313	-1.108	-0.2822
Dry gas						
Hydrogen	2.016	0.33	27.143	92.748×10^{-4}	-0.1381	0.78451
Methane	16.043	0.34	19.251	52.126×10^{-3}	0.11974	-1.132
Ethane	30.070	0.33	-5.409	0.17811	-0.60938	0.087127

Table 6: Constants in specific heat capacities of components in LPG and dry gas.

The molecular weights of gasoline, LPG and dry gas were calculated from the weight fractions and molecular weights of the components in the lump from Tables 4-6 to be 114.7149, 51.9521 and 16.043 kg/kmol, respectively while the molecular weight of steam is 18.0 kg/kmol. In Tables 3, 4, 6, the specific heat capacity of the component is expressed thus:

$$c_p = a + bT + cT^2 + dT^3 \quad (49)$$

which is expressed in J/(mol K).

In Table 5, the specific heat capacities of other components in gasoline obtained from ASPEN PLUS/HYSYS 9.0 are in the form:

$$c_p = a + bT + cT^2 + dT^3 + eT^4 + fT^5 + gT^6 \quad (50)$$

which is expressed in kJ/(kg K).

So, the specific heat capacity of gasoline as a lump, $c_{p,GA}$, is given by:

$$c_{p,GA} = \underbrace{\sum_{j=1}^{32} m_j c_{pj}}_{using\ equation(49)} + \underbrace{M_{GA}\sum_{j=33}^{37} m_j c_{pj}}_{using\ equation(50)} \quad (51)$$

which is now expressed in J/(mol K).

The specific heat capacity of LPG was computed using:

$$c_{p,LPG} = m_{C_3H_8} c_{p,C_3H_8} + m_{C_4H_{10}} c_{p,C_4H_{10}} \quad (52)$$

The specific heat capacity of DG was computed using:

$$c_{p,DG} = m_{H_2} c_{p,H_2} + m_{CH_4} c_{p,CH_4} + m_{C_2H_6} c_{p,C_2H_6} \quad (53)$$

The specific heat capacity of coke, which is taken to be carbon – graphite, was obtained from Smith, et al. [48] as:

Copyright© Olafadehan OA, et al.

$$c_{p,CK} = R_u\left(1.771 + 7.71\times10^{-4}T - 8.67\times10^{4}T^{-2}\right)$$ J/(mol K) (54)

while the specific heat capacity of steam is given thus: (Smith. et al.[48]):

$$c_{p,stm} = R_u\left(3.470 + 1.450\times10^{-3}T + 1.21\times10^{4}T^{-2}\right)$$ J/(mol K) (55)

The specific heat capacity of catalyst does not change with temperature during reaction, and its value is (Ahari et al., 2008): $c_{p,cat} = 1.087$ kJ/(kg K). The viscosity of VGO was estimated using the correlations obtained from ASPEN PLUS/HYSYS 9.0:

$$\mu_{VGO} = -6.0029\times10^{-7} + 1.2294\times10^{-8}T - 1.3150\times10^{-12}T^{2} + 6.4680\times10^{-17}T^{3}$$ (56)

where T is in K and the viscosities are expressed in Ns/m^2.

In order to account for temperature effect in the riser reactor, the specific heat capacity of each lump in the reaction network for the catalytic cracking of vacuum oil gas expressed as function of temperature was then introduced into the model equations as demanded. This is in variance with previous works in the literature.

The kinetic and thermodynamic parameters for the catalytic cracking of vacuum gas oil in the CNPC FCCU riser reactor are given in Table 7, which were used for simulation.

Parameters	Frequency factor, $(k_{i,j})_0$	Activation Energy, $E_{i,j}$ (J/mol)	Heat of Reaction, $(\Delta H_{rxn})_i$ (J/mol)
$k_{1,2}$	6712.72	50727	-40970
$k_{1,3}$	219000	70000	-46960
$k_{1,4}$	637.87	59750	317440
$k_{1,5}$	1869	176440	790600
$k_{1,6}$	1546.40	59750	633300
$k_{2,3}$	240.46	57500	3600
$k_{2,4}$	46.08	141950	212570
$k_{2,5}$	3560	81780	493340
$k_{2,6}$	281.68	59750	400080
$k_{3,4}$	40.39	74220	111190
$k_{3,5}$	1.6	135340	255590
$k_{3,6}$	15.60	59750	42420
$k_{4,5}$	78.98	89270	57240
$k_{4,6}$	296.4	31500	2100

Table 7: Kinetic and thermodynamic parameters used for riser reactor types of FCCU simulation [2,19]. For feedstock cracking, the units of $(k_{i,j})_0$ are wt. fraction./s while for other lump cracking, the units of $(k_{i,j})_0$ are s^1 .

Parameters	Value
Riser Height, H_R	32.8 m
Riser inner diameter, D_R	0.6 m
Particle density, ρ_p	1500 kg/m^3
Particle mean diameter, D_p	60 m
Gaseous phase density, $(\rho_g)_0$	1.3 kg/m^3
Gas viscosity, μ	2×10^{-5}Pa.s
Solids circulation rate, G_s	22 kg/(m^2 s)

Table 8: Operational conditions of industrial riser reactor considered [49].

Copyright© Olafadehan OA, et al.

Table 8 provides information on the configuration of the industrial plant as reported by Souza, et al. [49]. Other parameter values used for numerical simulation are given in Table 9.

Parameter	Values	References
Feedstock		
Vacuum Gas Oil mass flow rate, F_{VGO}	12744 kg/h	Souza, et al. [49]
Steam mass flow rate, F_{stm}	442.4 kg/h	Souza, et al. [49]
Steam inlet temperature, T_{stm}	320°C	Souza, et al. [49]
Feed inlet temperature, T_{VGO}	320°C	Souza, et al. [49]
Flow rate of catalyst, F_{cat}	62445.6 kg/h	Souza, et al. [49]
Catalyst inlet temperature, T_{cat}	567°C	Souza, et al. [49]
Riser pressure, p_{in}	2.5 bar	Souza, et al. [49]
Catalyst to oil ratio (COR)	4.9	Souza, et al. [49]
Physical properties		
Specific heat capacity of liquid feed, $c^{L}_{p,VGO}$	2670 J/kg	Ahari, et al. [50]
Specific heat capacity of vapour feed, $c^{V}_{p,VGO}$	3300 J/kg	Ahari, et al. [50]
Catalyst density, ρ_{cat}	1560 kg/m^3	Souza, et al. [49]
Gas phase viscosity, μ_{gas}	2×10^{-5}Pa.s	Souza, et al. [49]
Particle density, ρ_p	1500 kg/m^3	
Vaporization temperature of feed, T_{vap}	698 K	Ahari, et al. [50]
Enthalpy of vaporization, ΔH_{vap}	190 kJ/kg	Ahari, et al. [50]
Specific heat capacity of steam, $c_{p,stm}$	2.0 kJ/kg K)	Souza, et al. [49]
Pore diameter	2 nm	Olanrewaju, et al. [51]
Particle diameter, D_p	60 µm	Olanrewaju, et al. [51]
Particle tortuosity, τ	7.0	Missen, et al. [52]
Heat transfer coefficient, h	1×10^3 kW/(m^2 K)	Souza, et al. [49]

Table 9: Other operating conditions of riser reactors of FCCU.

Due to the dearth of some data from the China National Petroleum Corporation, data were obtained from a similar Refinery investigated by Souza, et al. [49] and Ahari, et al. [50] , as indicated in Table 9 for computational purposes.

Estimation of Effective Diffusivity and Mass and Heat Transfer Coefficients

The mass transfer coefficient, k_g, was calculated from the j_D factor and the Schmidt's number ([35])::

$$k_g = \frac{j_D G_V}{\rho_g \phi_p} Sc^{-2/3} \quad (57)$$

$$Sc = \frac{\mu_g}{D_k \rho_g} \quad (58)$$

The heat transfer coefficient, h_{gs}, was calculated from the j_H factor and the Prandtl's number, Pr, (Smith [35]):

$$h_{gs} = \frac{j_H c^V_{p,VR} G_V}{\phi_p} \Pr^{-2/3} \quad (59)$$

$$\Pr = \frac{c^V_{p,VR} \mu_g}{k_{cat}} \quad (60)$$

The effective diffusivity, D_e, was calculated from the Knudsen diffusivity (Fogler [53]):

$$D_e = \frac{D_k \phi_p \sigma_c}{\tau} \quad (61)$$

The Knudsen diffusivity, D_k, was estimated thus (Smith [35]):

Copyright© Olafadehan OA, et al.

$$D_k = \frac{d_{pore}}{3}\sqrt{\frac{8R_u T_g}{1000\pi \overline{M}_g}} \quad (62)$$

In the fluidized bed catalytic reactor, the *j*-factors (j_D and j_H) are approximately equal and was estimated using the correlation given thus (Smith, et al. [48]):

$$j_D, j_H = 1.77\left|\frac{d_p G_V}{\mu_g\left(1-\in_g\right)}\right| \quad (63)$$

Simulation Results and Discussion

The assignin and evalin MATLAB R2017a functions were used to call out the values of the interstitial gas velocity, while the gas phase mass flow rate, superficial velocity, average molecular weight and density were calculated using the results from the code. The simulated results of the developed mathematical models for riser reactor of CNPC FCCU without mass and heat transfer resistances did not match any of the plant data at all as the results were unrealistic, especially for the weight fraction of each lump being negative. Hence, the results were not presented here and neither was discussions made in that respect. Only the simulated results with the incorporation of mass and heat transfer resistances in the developed models were presented and discussed, as these results show promising results, as presented in Figures 3-12. In Figures 3-5, comparison was made between the actual plant data of the VGO and product yields with simulated results for both instantaneous and one-dimensional vaporization of feedstock, and summarized in Table 10. Excellent agreements were achieved between the CNPC-FCCU riser reactor exit yield of VGO, diesel, gasoline, LPG, dry gas and coke and the predicted values considering instantaneous vaporisation of feedstock with maximum % error being ± 2.41, where optimal yields of the cracked products needed to meet market demands and ensuring maximum profit were achieved. Moreover, our predicted values of the major important riser reactor weight fractions of diesel and gasoline: 0.180319 and 0.471354 compared exceedingly well with those obtained by John, et al. [17]: 0.1842 and 0.4863, with % error being ± 2.15 and ± 3.17 respectively using instantaneous vaporization of feedstock. However, the simulated results in terms of exit yield of each lump did not match the plant data except for the VGO exit yield and conversion using one-dimensional vaporisation of feedstock model. The % errors in this case were all greater than 5 with the exception of the yield of VGO with % error being ± 3.13. Hence, instantaneous vaporisation of feedstock must have occurred at the entrance of the riser reactor. Moreover, it is evident in Figure 3 that almost 75% conversion of VGO occurs in the first 10 m of the riser reactor. This agrees with literature findings and it can be inferred that the rate of cracking is fastest at the entrance into the riser reactor (Theologos and Markatos, [54]; Martin, et al. [55]; Kimm, et al. [56]; Ali, et al. [31]; Derouin, et al. [57]; Berry, et al. [58]; Xu, et al. [59]; Heydari, et al. [18]; Olafadehan, et al. [20]). Also, for both instantaneous and one-dimensional vaporization of feedstock, most of the conversion occurs in the first-third of the riser reactor, implying that, giving a head-room of another 5 m for catalytic cracking of VGO to occur and for transportation of the products out of the riser reactor, then almost the second half of the riser reactor is redundant. Probably there is no need for the construction of the height of the riser reactor to be 32.8 m for the commercial CNPC as espoused in one of our studies for the Khartoum Refinery Company (Olafadehan, et al. [20]). The predicted results for one-dimensional vaporisation of feedstock yielded poor results. Hence, instantaneous vaporisation of feedstock must have occurred at the entrance of the riser reactor.

Lump	Plant data	Instantaneous Vaporization		One-dimensional Vaporization	
	Yield (wt %)	Yield (wt %)	% error	Yield (wt %)	% error
VGO	8.00	7.8673	± 1.66	8.25	± 3.13
Diesel	17.80	18.0319	± 1.30	19.4875	± 9.48
Gasoline	48.30	47.1354	± 2.41	44.1354	± 8.62
LPG	19.02	19.4484	± 2.25	22.3103	± 17.30
Dry gas	1.95	1.9295	± 1.05	1.3107	± 32.78
Coke	4.93	5.02	± 1.83	5.8899	± 19.47

Table 10: Comparison of the plant exit yield form the riser reactor of CNPC FCCU with simulated results.

Copyright© Olafadehan OA, et al.

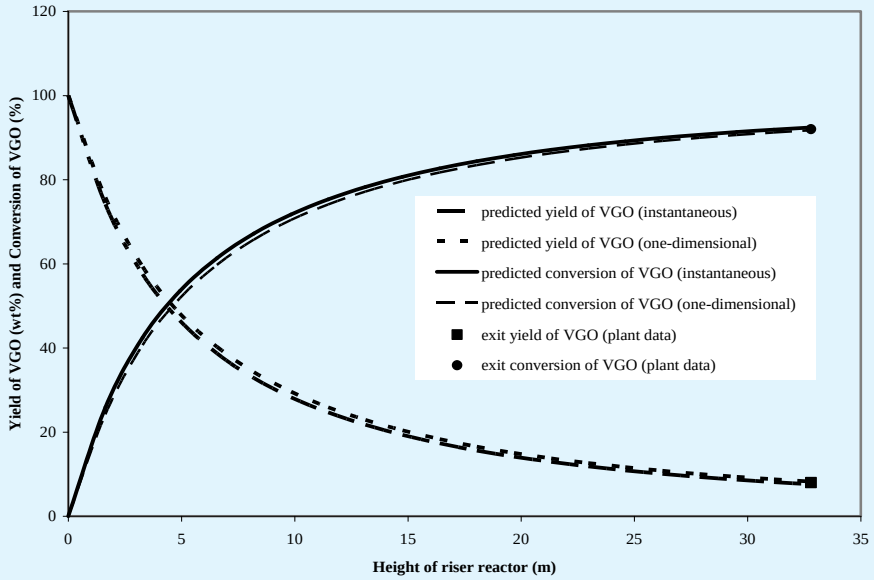

Figure 3: Yield and conversion of VGO along height of riser reactor for instantaneous and one-dimensional vaporization of feedstock.

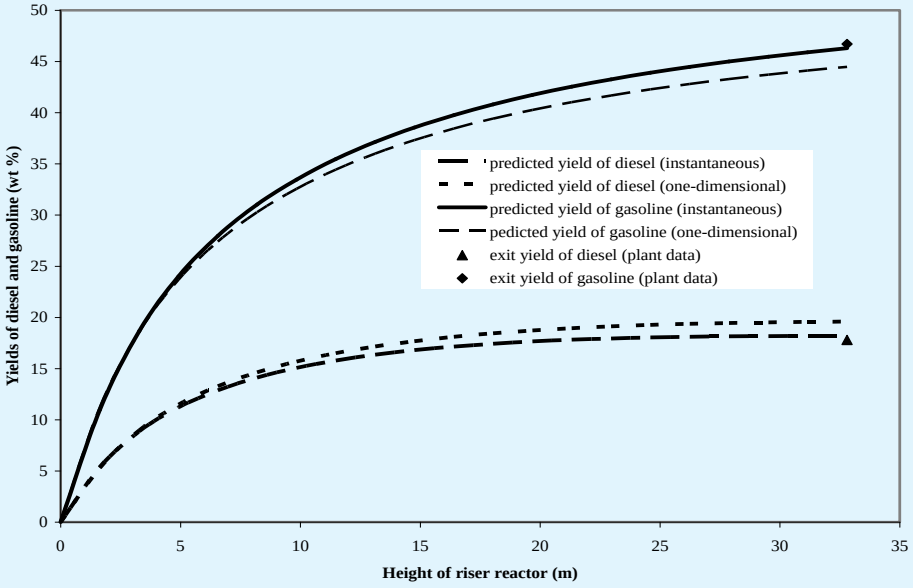

Figure 4: Yield of diesel and gasoline along height of riser reactor for instantaneous and one-dimensional vaporization of feedstock.

Copyright© Olafadehan OA, et al.

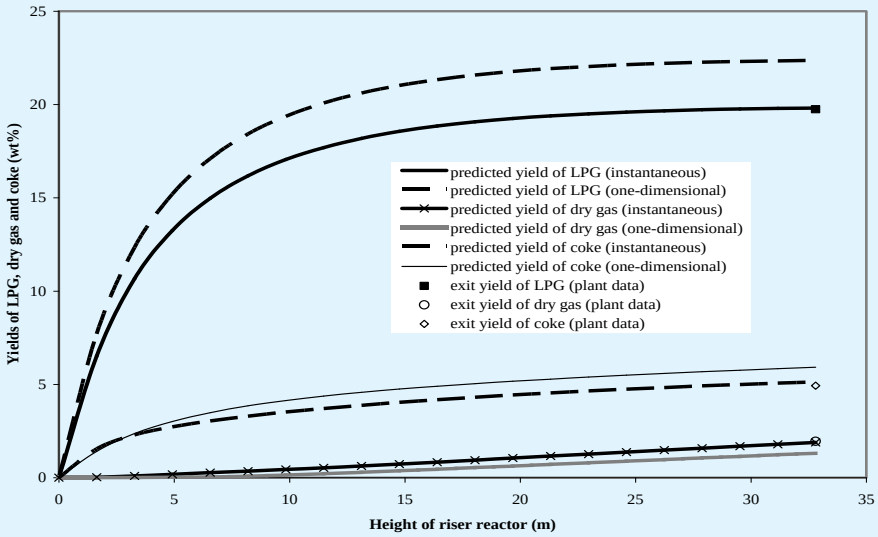

Figure 5: Yields of LPG, dry gas and coke along height of riser reactor for instantaneous and one-dimensional vaporization of feedstock.

Figure 6 shows the catalyst and gas phase residence times in the riser reactor for both instantaneous and one-dimensional vaporization of feedstock. The gas residence time is 7.8 s for both vaporization models. Since the catalyst is heavier than the gas, it stays about 13 s inside the riser reactor for both vaporization models.

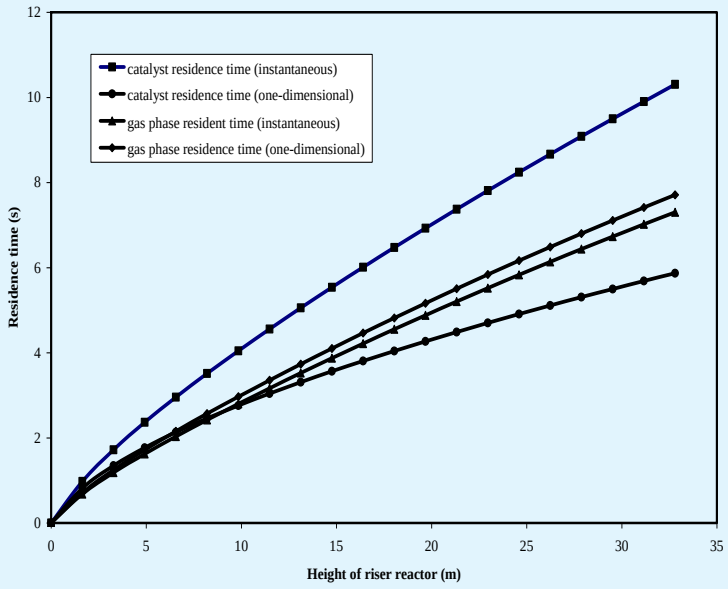

Figure 6: Catalyst and gas phase residence times along height of riser reactor for instantaneous and one-dimensional vaporization of feedstock.

Copyright© Olafadehan OA, et al.

Figures 7 and 8 show the respective gas and solid phases' temperature profiles along the height of the riser reactor for both instantaneous and one-dimensional vaporization of feedstock. The atomization of feed into fine drops facilitated high rates of heat transfer between catalyst and feed. This resulted in a rapid fall in the cluster phase temperature in the first few metres of the riser reactor entry zone as it loses heat to hydrocarbon feed for both cases of vaporization. Within the same bottom zone, the gas phase temperature increased quickly until both the gas and solid phases attained thermal equilibrium, which remained constant for the remaining height of the riser reactor. This is indicative of the fact that most of the reactions occurred at the bottom of the riser. A predicted outlet temperature of 747.75 K was obtained for instantaneous vaporisation of feedstock, which was in excellent agreement with plant exit temperature of 750 K, with % error being $\pm$ 0.3. However for the case of one-dimensional vaporization of feedstock, predicted exit temperature of 728.88 K revealed a somewhat agreement with the plant data since % error was $\pm$ 2.82. The higher temperature for the instantaneous vaporisation resulted in a higher feedstock conversion of 0.5% more than that for the one-dimensional model.

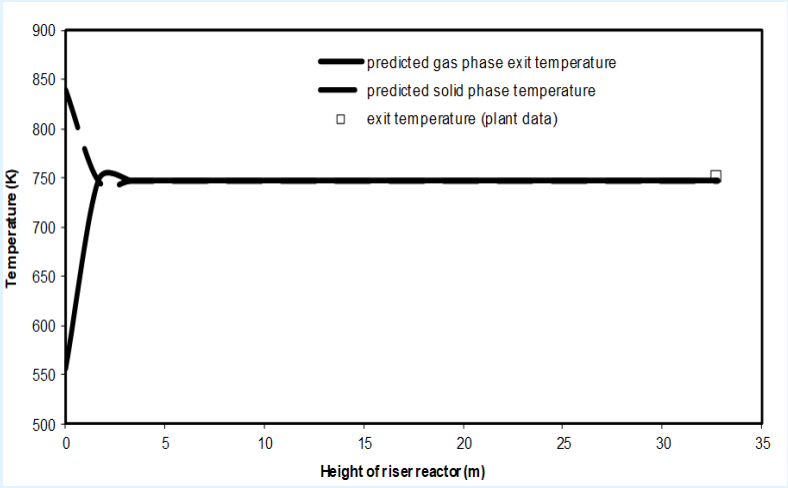

Figure 7: Temperature profile along height of riser reactor for instantaneous vaporization of feedstock.

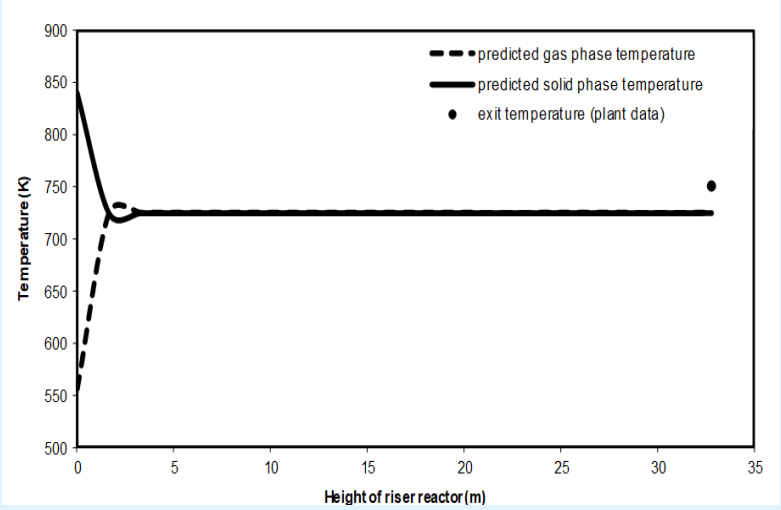

Figure 8: Temperature profile along height of riser reactor for one-dimensional vaporization of feedstock.

Copyright© Olafadehan OA, et al.

The predicted pressure profiles along the height of the riser reactor for both instantaneous and one-dimensional vaporization of the feedstock are shown in Figure 9. The predicted pressure drops in the CNPC FCCU riser reactor were 46.621 kPa and 43.289 kPa for instantaneous and one-dimensional vaporisation of feedstock respectively, which are in agreement with the actual pressure drop of 35-62 kPa that exists in commercial FCCU riser reactors (Sadeghbeigi [60]).

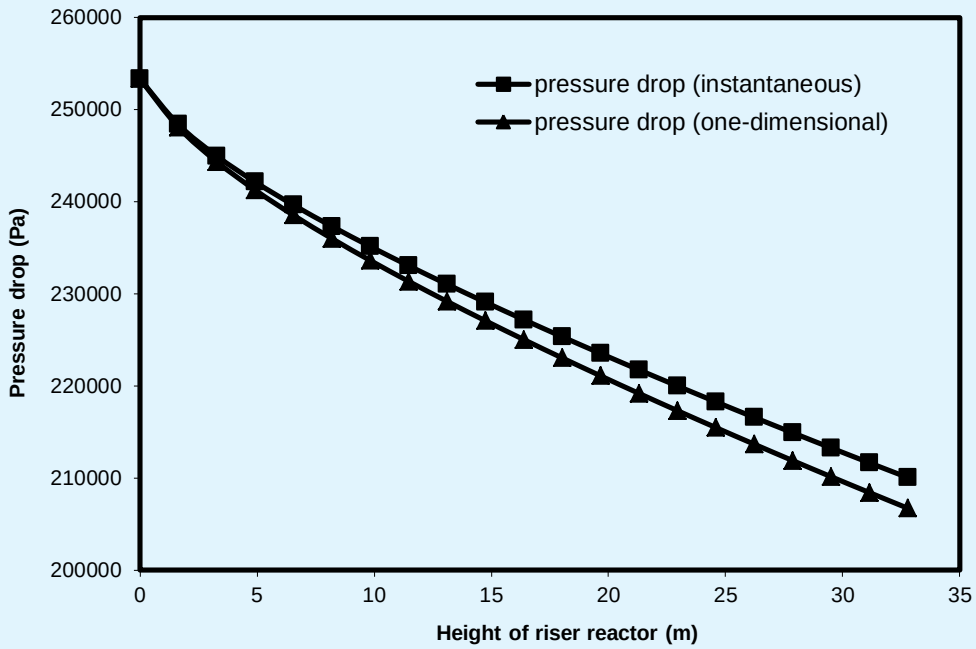

Figure 9: Pressure profile along height of riser reactor for instantaneous and one-dimensional vaporization of feedstock.

The cluster and gas phase velocity profiles and the slip factor variation along height of riser reactor for both vaporization models of instantaneous and one-dimensional are depicted in Figures 10-12 respectively. The slip factor is high at the beginning of the riser reactor indicating the gas velocity is much greater than the particle velocity. High catalyst temperature caused high catalyst loading which further causes slower vaporisation rates and low gas velocities initially. Hence, the gas phase velocity first decreases within about 2 m of the riser reactor due to deceleration when it contacts the regenerated catalyst, and it then increases owing to cracking reactions. The gas accelerates the catalyst, which thus resulted in a decrease in slip factor as shown in Figure 12. The slip factor values may range from 1.2 to 4, where 2 is considered typical in a commercial FCCU (Fernandes, et al. [38]). In this study, the slip factor ranged from 1 to 2.6. Figures 10 and 11 show that the gas phase and solid phase velocities are at maximum values toward the riser reactor exit. In Figures 10 and 11, lower velocities of the solid and gas phases were obtained using one-dimensional valorisation of feedstock throughout the riser reactor than does the instantaneous vaporisation model, as the vaporization does not take place at once.

Copyright© Olafadehan OA, et al.

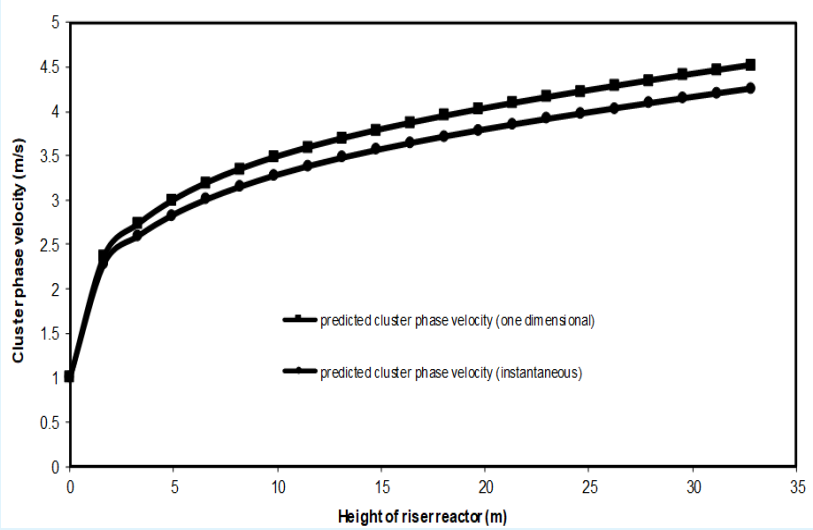

Figure 10: Cluster phase velocity profile along height of riser reactor for instantaneous and one-dimensional vaporization of feedstock.

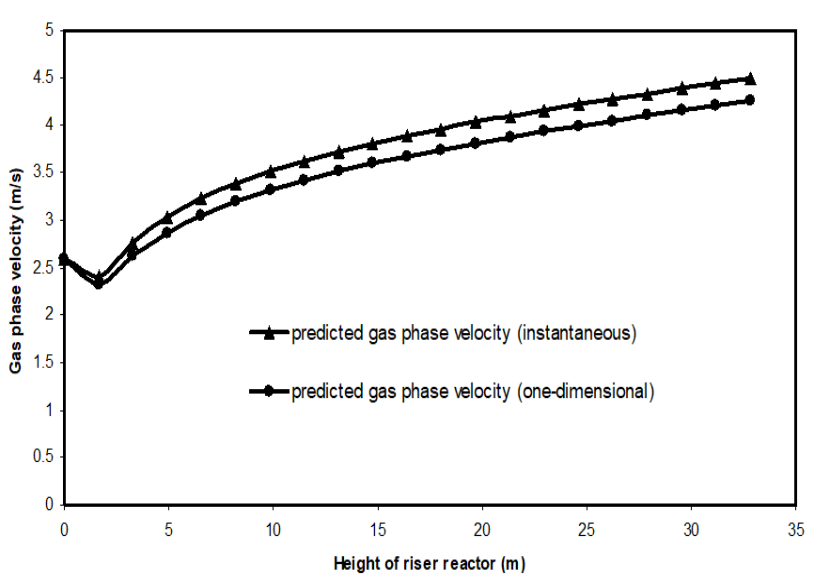

Figure 11: Gas phase velocity profile along height of riser reactor for instantaneous and one-dimensional vaporization of feedstock.

Copyright© Olafadehan OA, et al.

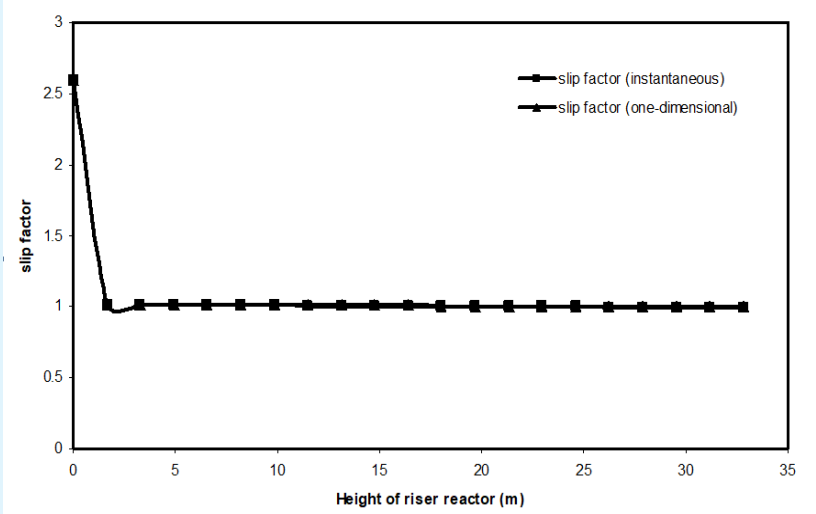

Figure 12: Variation of slip factor along height of riser reactor for instantaneous and one-dimensional vaporization of feedstock.

Figure 13 shows the variation of gas phase voidage along height of riser reactor for instantaneous and one-dimensional vaporization of feedstock. This is an indication of molar expansion of the gas phase as cracking occurs in the riser reactor. At about 3 m, the riser height is 85% occupied by the gas phase, and this agrees with the findings of Gauthier [61].

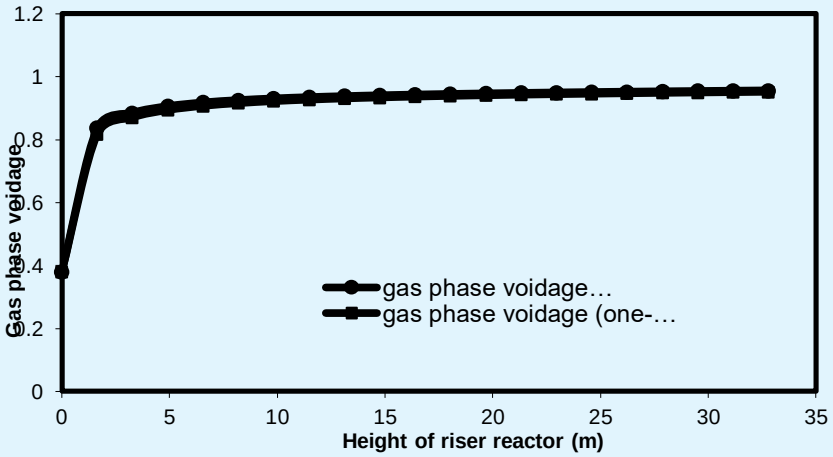

Figure 13: Gas voidage variation along height of riser reactor for instantaneous and one-dimensional vaporization of feedstock.

Figure 14 shows the variation of gas phase density along height of riser reactor for instantaneous and one-dimensional vaporization of feedstock. The gas phase molecular weight along the riser reactor height decreases due to the increase of light products percentage in the gas phase towards the riser exit. Consequently, the gas density decreases along the height of riser, as shown in Figure 14 for both vaporisation approaches of feedstock.

Copyright© Olafadehan OA, et al.

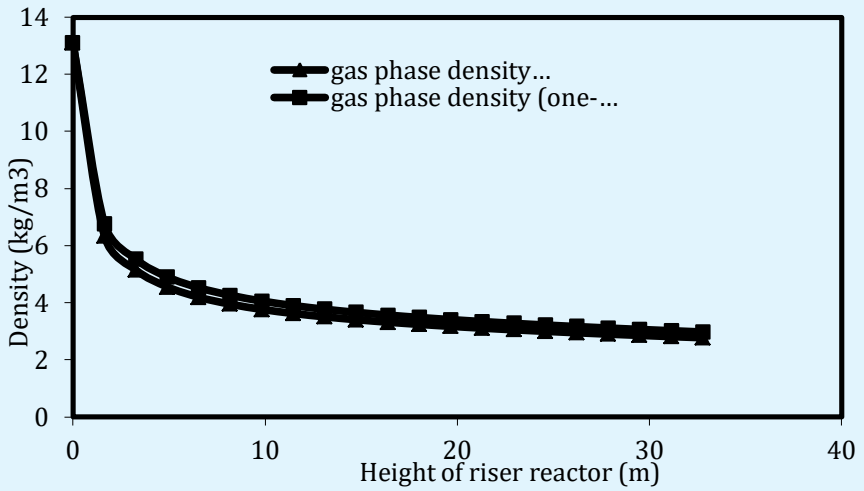

Figure 14: Gas phase density along height of riser reactor for instantaneous and one-dimensional vaporisation of feedstock.

Figure 15 shows deactivation function of catalyst and concentration of coke on catalyst surface along height of riser reactor for instantaneous and one-dimensional vaporization of feedstock. The deactivation function decreased along riser reactor height due to the fact that the catalyst was fresh and its activity was unity before catalytic cracking occurred in the riser reactor. As catalytic reaction progresses, the catalyst activity decreases along the height of riser owing to the deposition of coke on the catalyst, thereby poisoning the active sites of the catalyst. Coke is being continuously generated along the height of the riser reactor so the coke concentration on the catalyst surface increases as depicted in Figure 15. Figure 16 shows deactivation function of catalyst against concentration of coke on the catalyst surface for instantaneous and one-dimensional vaporisation of feedstock. It is evident that deactivation function decreases with increasing concentration of coke on the catalyst surface.

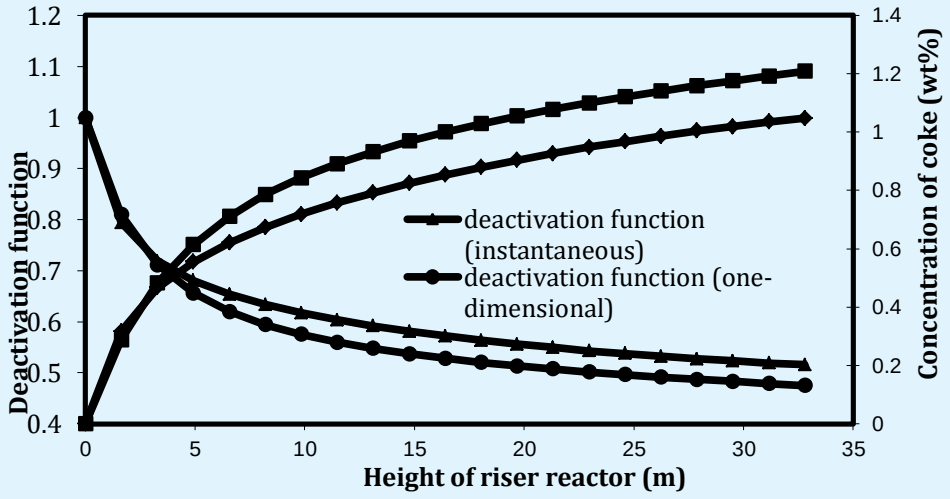

Figure 15: Deactivation function and concentration of coke along height of riser reactor for instantaneous and one-dimensional vaporization of feedstock.

Copyright© Olafadehan OA, et al.

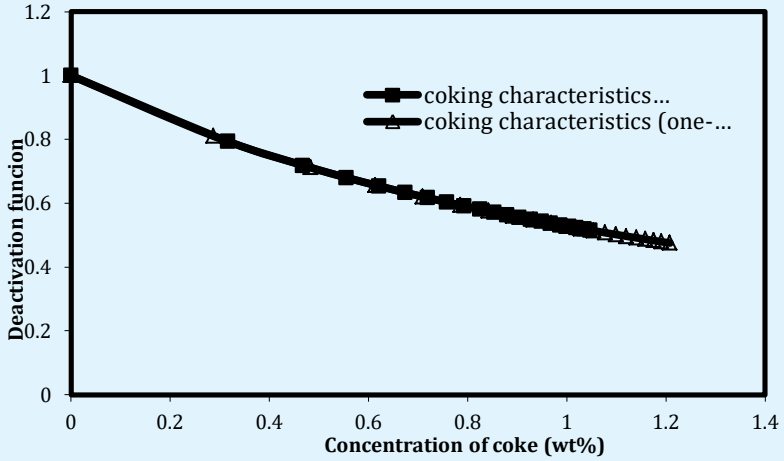

Figure 16: Deactivation function of catalyst against concentration of coke on the catalyst surface for instantaneous and one-dimensional vaporization of feedstock.

Figure 17 shows the comparison of the effectiveness factor for first and second orders conversion of VGO using instantaneous and one-dimensional vaporization of feedstock. For the former, the effectiveness factor for first order VGO conversion ranged from 0.03688 (at the riser inlet) to 0.03596 (at the reactor outlet). It ranged from 0.03688 (at the riser inlet) to 0.03696 (at the riser outlet) for second order VGO conversion. However, for the one-dimensional vaporisation, the effectiveness factor ranged from 0.03687 (at the riser inlet) to 0.03617 (at the riser outlet) for first order conversion of VGO while it ranged from 0.03687 (at the riser inlet) to 0.03697 (at the riser outlet) for second order VGO conversion. These results reveal that the effectivess factor does not change significantly along the height of riser reactor, thereby justifing the assumption of the same effectiveness factor for both first and second order, as given in Equation (5): the maximum deviation along the riser reactor height is negligible (0.00079).

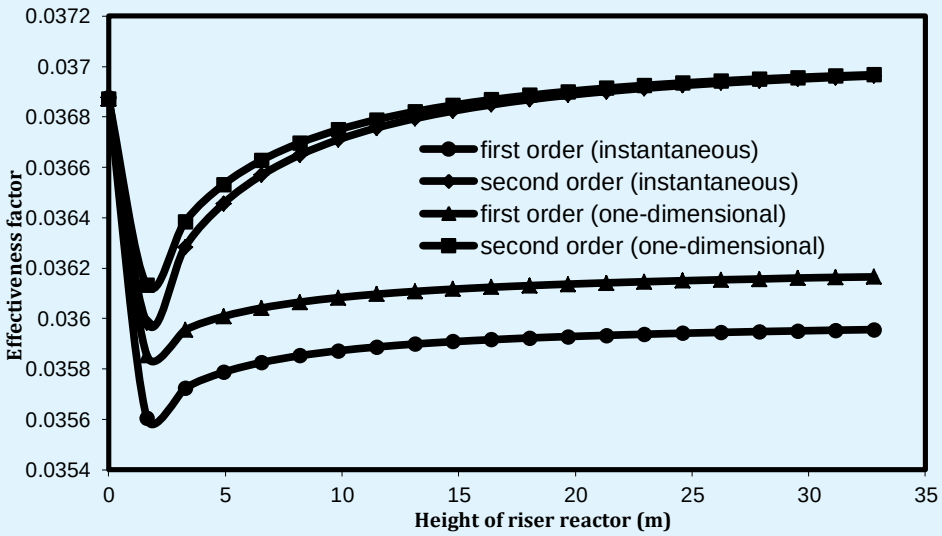

Figure 17: Comparison of the effectiveness factors for first and second order conversion of VGO for instantaneous and one-dimensional vaporisation of feedstock.

Copyright© Olafadehan OA, et al.

Conclusion

A one-dimensional adiabatic mathematical model of an industrial fluid catalytic cracking unit riser reactor was presented. The model combined the two-phase hydrodynamic model of the reactor and the catalyst deactivation model with the six-lump kinetics of catalytic cracking of vacuum gas oil. An important contribution of this study was the inclusion of the viscosities and the specific heat capacities of gas oil and the lump components as a function of temperature in the developed model, which were usually assumed to be constant in most previous works. Moreover, diffusion resistance and heat transfer were incorporated into the kinetic model, which is a deviation from the general norm in the literature. Two vaporization approaches of instantaneous and one-dimensional were considered. The resulting models consist of 11 highly non-linear, stiff and coupled ordinary differential equations, which was a chief advantage for the fact that the governing equations for the FCCU riser reactor did not include any partial differential equations. This facilitated the numerical solution of the equations using the MATLAB 2017a buit0in function ode23tb, made the model particularly suitable for control studies and real time optimization. Simulation studies were performed to investigate the effect of changing various process variables. Our results revealed that the vaporization model had significant influence on the product composition at the riser outlet. Also, feedstock (VGO) conversions of 92.81% and 92.32% were predicted by the developed model in this study for the instantaneous and one-dimensional model respectively. Excellent agreements were equally achieved between the plant data and the predicted yield of the lump and the exit riser reactor temperature for instantaneous vaporization of feedstock, with % error < 5. Consequently, instantaneous vaporization of the feedstock might have occurred at the inlet of the riser reactor. Moreover, our study revealed that almost half of the riser is redundant during the catalytic process and thus the designer of industrial/commercial FCCU-riser reactor should consider reducing the height of the riser in order to save operating cost in terms of the cost of construction of materials. Finally, the excellent results obtained with the developed model reveal that it is possible to integrate the proposed model in a dynamic model of a FCCU-riser reactor for use in subsequent studies of control and real time optimization.

NOTATION

AAD	average absolute deviation
COR	catalyst to oil weight ratio
D_c	cluster diameter, m
D_R	riser reactor, m
$E_{i,j}$	activation energy for the reaction of lump *i* to lump *j*, J/mol
F_c	mass flow rate of cluster phase, kg/s
F_i	mass flow rate of component *i*, kg/s
f_s	solid friction factor
G_c	mass flux of cluster phase (catalyst+coke), kg/(m^2 s)
G_v	mass flux of gas phase (VGO+steam), kg/(m^2 s)
ΔH_{vap}	vacuum gas oil enthalpy of vaporization, J/kg
j_D	*j*-factor for mass transfer, dimensionless
j_H	*j*-factor for heat transfer, dimensionless
k_g	mass transfer coefficient between the bulk gas and solid surface, $m_f^3/\left(m_p^2 s\right)$
$\left(k_{i,j}\right)_0$	frequency factor for the reaction of lump *i* generating lump *j*, s^{-1}
k_A	adsorption coefficient of heavy aromatics, dimensionless
k_N	deactivation coefficient of basic nitrogen poisoning, dimensionless
R_u	universal gas constant, J/(mol K)
S_a	surface area of the catalyst per unit mass of catalyst, m^2/kg cat
Sc	Schmidt's number, dimensionless
S_v	true weight hourly space velocity, s^{-1}
t	contact time of oil vapour with catalyst, s
T	riser temperature, K
T_c	cluster phase temperature, K
T_g	gas phase temperature, K
T_R	riser temperature, K

Copyright© Olafadehan OA, et al.

$\bar{v}_c$ dimensionless cluster phase velocity in the riser

$(v_c)_0$ initial cluster phase velocity in the riser, m/s

y_A wt% of aromatics in feedstock

y_{ASP} wt% of asphaltene in feedstock

y_N wt% of basic nitrogen in feedstock

y_R wt% of resins in feedstock

Greek Symbols

$\in_b$ void fraction of bed, dimensionless

σ dimensionless riser reactor height $(= z/H_R)$

ρ_c density of cluster phase (catalyst+coke) in the riser, kg/m^3

ρ_p density of solid particles (catalyst+coke) in the riser, kg/m^3

Subscripts

CK	coke lump
cat	catalyst
D	diesel lump
DG	dry gas
GA	gasoline lump
LPG	liquefied petroleum gas lump
s	solid
sf	solid friction
stm	dispersion steam
VGO	vacuum gas oil lump

Superscripts

L	liquid
V	vapour

References

1. Xiong K, Lu C, Wang Z, Gao X (2015) Kinetic Study of Catalytic Cracking of Heavy Oil over an In-situ Crystallized FCC Catalyst. Fuel 142: 65-72.

2. Du YP, Yang Q, Zhao H, Yang CH (2014) An Integrated Methodology for the Modeling of Fluid Catalytic Cracking (FCC) Riser Reactor. Appl Petrochem Res 4(4): 423-433.

3. Popa C (2014a) Application of Plantwide Control Strategy to the Catalytic Cracking Process. Procedia Eng 69: 1469-1474.

4. Popa C (2014b) Four-Lump Kinetic Model vs. Three-Lump Kinetic Model for the Fluid Catalytic Cracking Riser Reactor. Procedia Eng 100: 602-608.

5. Gupta RK, Kumar V, Srivastava V (2007) A New Generic Approach for the Modelling of Fluid Catalytic Cracking (FCC) Riser Reactor. Chem Eng Sci.62(17): 4510-4528.

6. Weekman V (1968) A Model of Catalytic Cracking Conversion in Fixed, Moving and Fluid-Bed reactors. Ind Eng Chem Proc Des 7(1): 90-95.

7. Weekman VW, Nace DM (1970) Kinetics of Catalytic Cracking Selectivity in Fixed, Moving and Fluid Bed Reactors. AIChE J 16(3): 397-404.

8. Weekman VW (1969) Kinetics and Dynamics of Catalytic Cracking Selectivity in Fixed Bed Reactors. Ind Eng Chem Proc Des Dev 8(3): 385-391.

9. Lee LS, Chen YW, Huang TN, Pan WY (1989) Four-Lump Kinetic Model for Fluid Catalytic Cracking Process. Can J Chem Eng 67(4): 615-619.

10. Lee LS, Yu SW, Cheng CT, Pan WY (1988) Fluidized-Bed Catalyst Cracking Regenerator Modelling and Analysis. The Chemical Engineering Journa 40(2): 71-82.

11. Gianetto A, Faraq H, Blasetti A, de Lasa H (1994) Fluid Catalytic Cracking Catalyst for Reformulated Gasoline's Kinetic Modeling. Ind Eng Chem Res. 33(12): 3053-3062.

12. Yen LC, Wrench RE, Ong AS (1988) Reaction Kinetic Correlation Equation Predicts Fluid Catalytic Cracking Coke Yields. Oil Gas J 86(2): 67-70.

13. Corella J, Frances E (1991) On the Kinetic Equation of Deactivation Cracking Commercial (FCC) Catalysts with Commercial Feedstocks. Stud Surf Sci Catal 68: 375-381.

14. Bollas GM, Lappasa AA, Iatridisa DK, Vasalos IA (2007) Five-Lump Kinetic Model with Selective Catalyst Deactivation for the Prediction of the Product Selectivity in the Fluid Catalytic Cracking Process. Catal Today 127(1-4): 31-43.

15. Alexiadis VI, Heuchel M, Thybaut JW, Traa Y, Marin GB, et al. (2018) Model Based Analysis of the Effect of Ethylphenol Addition to n-decane in Fluid Catalytic

Copyright© Olafadehan OA, et al.

Cracking over an Extended Zeolite Library. ISCRE25 FLORENCE 2018 Bridging, Science and Technology, 25th International Symposium on Chemical Reaction Engineering.

16. Takatsuka T, Sato S (1987) A Reaction Model for Fluidized-Bed Catalytic Cracking of Residual Oil. Int Chem Eng 27(1): 107-116.

17. John YM, Mustafa MA, Raj Patel R, Mujtaba IM (2019) Parameter Estimation of a Six-Lump Kinetic Model of an Industrial Fluid Catalytic Cracking Unit. Fuel 235: 1436-1454.

18. Heydari M, Ale Ebrahim H, Dabir B (2010) Modeling of an Industrial Riser in the Fluid Catalytic Cracking Unit. Am J Appl Sci 7(2): 221-226.

19. Ahmed A, Maulud A, Ramasamy M, Lau KK, Mahadzir S (2014) 3D CFD Modelling and Simulation of RFCC Riser Hydrodynamics and Kinetics. J Appl Sci 14(23): 3172-3181.

20. Olafadehan OA, Sunmola OP, Jaiyeola A, Efeovbokhan V, Abatan OG (2018) Modelling and Simulation of an Industrial RFCCU-Riser Reactor for Catalytic Cracking of Vacuum Residue. App Petrochem Res 8(4): 219-237.

21. Ellis RC, Li X, Riggs JB (1998) Modeling and Optimization of a Model-IV Fluidized Catalytic Cracking Unit. AIChE. J 44(9): 2068-2079.

22. Hagelberg P, Eilos I, Hiltunen J, Lipiainen K, Niemi VM, et al. (2002) Kinetics of Catalytic Cracking with Short Contact Times. App Catal A: Gen 223(1-2): 73-84.

23. Jacob SM, Gross B, Voltz SE, Weekman VW (1976) A Lumping and Reaction Scheme for Catalytic Cracking. AIChE. J 22(4): 701-713.

24. Sa Y, Liang X, Chen X., Liu J (1995) Study of 13-lump kinetic model for residual catalytic cracking. Petrochem Eng Cor, pp: 145-152.

25. Barbosa AC, Lopez GC, Rosa LM, Mori M, Martigoni WP (2013) Three Dimensional Simulation of Catalytic Cracking Reactions in an Industrial Scale Riser using a 11-Lump Model. AIDIC Conference Series 11: 31-40.

26. Oliveira L, Biscaia EC (1989) Catalytic Cracking Kinetic Models. Parameter Estimation and Model Evaluation. Ind Eng Chem Res 28(3): 264-271.

27. Pitault I, Nevicato D, Forissier M, Bernard JR (1994) Kinetic Model on a Molecular Description for Catalytic Cracking of Vacuum Gas Oil. Chem Eng Sci 49(24): 4249-4262.

28. Pinheiro CI, Fernandes JL, Domingues L, Chambel AJ, Graca I, et al. (2011) Fluid Catalytic cracking (FCC) Process Modeling, Simulation, and Control. Ind Eng Chem Res 51(1): 1-29.

29. Hu Y, Xu W, Hou W, Su H, Chu J (2005) Dynamic Modelling and Simulation of a Commercial Naphtha Catalytic Reforming Process. Chin Chem Eng 13: 74-82.

30. Liu Z, Meng X, Xu C, Gao J (2007) Secondary Cracking of Gasoline and Diesel from Heavy Oil Catalytic Pyrolysis. Chin J Chem Eng 15(3): 309-314.

31. Ali H, Rohani S, Corriou JP (1997) Modeling and Control of a Riser Type Fluid Catalytic Cracking (FCC) Unit. Trans Inst Chem Eng 75: 380-395.

32. Arandes JM, Lasa HI (1992) Simulation and Multiplicity of Steady States in Fluidized FCCUs. Chem Eng Sci 47(9-11): 2535-2540.

33. Arbel A, Huang Z, Rinard IH, Shinnar R, Sapre AV (1995) Dynamic and Control of Fluidized Catalytic Crackers.1.Modeling of the Current Generation of FCC's. Ind Eng Chem Res 34(4): 1228-1243.

34. Han IS, Chung CB (2001) Dynamic Modelling and Simulation of a Fluidized Catalytic Cracking Process. Part II: Property Estimation and Simulation. Chem Eng Sci 56(5): 1973-1990.

35. Smith JM (1981) Chemical Engineering Kinetics. 3rd(Edn.), McGraw-Hill, New York.

36. Chen JW, Cao HC (2005) Catalytic Cracking Technology and Engineering; China Petrochemical Press: Beijing, China.

37. Tsuo YP, Gidaspow D (1990) Computation of Flow Patterns in Circulating Fluidized Beds. AIChE J 36(6): 885-896.

38. Fernandes JL, Verstraete JJ, Pinheiro CI, Oliveira, NM, Ribeiro FR (2007) Dynamic Modelling of an Industrial R2RFCC Unit. Che Eng Sci 62(4): 1184-1198.

Copyright© Olafadehan OA, et al.

39. Bromley LA, Wilke CR (1951) Viscosity Behaviour of Gases. Ind Eng Chem 43(7): 1641-1648.

40. American Petroleum Institute (API) (1992) Technical Data Book: Petroleum Refining. 5th(Edn.), New York.

41. Daubert TE, Danner RP (1985) Data Compilation Tables of Properties of Pure Components, American Institute of Chemical Engineers, New York.

42. Pugsley TS, Berruti F (1995) A Core-Annulus Solids Interchange Model for Circulating Fluidized Bed and FCC risers. Tours: Fluidization VIII Preprints, pp: 449-455.

43. Pugsley TS, Berruti F (1996) A Predictive Hydrodynamic Model for Circulating Fluidized Bed Risers. Powder Technol 89(1): 57-69.

44. Konno H, Saito SJ (1969) Pneumatic Conveying of Solids through Straight Pipe. J Chem Eng J 2(2): 211-217.

45. Blasius H (1913) Grenzschichten in Flussigkeiten Mit Kleiner Reibung. Mitt Forschungsarb 131: 1-39.

46. Negrao CO, Baldessar F (2006) Simulation of Fluid Catalytic Cracking Risers–A Six Lump Model. The 11th Brazillian Congress of Thermal Sciences and Engineering, Curitiba, Brazil.

47. Sinnott R, Towler G (2013) Chemical Engineering Design. Volume 6, 5th(Edn.), Butterworth-Heinemann (An imprint of Elsevier), Oxford and USA.

48. Smith JM, Van Ness HC, Abbott MM (2001) Introduction to Chemical Engineering Thermodynamics. 6th(Edn.), McGraw-Hill Inc.

49. Souza JA, Vargas JVC, Von Meien OF, Martignoni W, Amico SC (2006) A Two-Dimensional Model for Simulation, Control and Optimization of FCC Risers. AIChE J 52(5): 1895-1905.

50. Ahari JS, Farshi A, Forsat K (2008) A Mathematical Modeling of the Riser Reactor in Industrial FCC Unit. Petroleum and Coal 50(2): 15-24.

51. Olanrewaju OF, Okonkwo PC, Aderemi BO (2015) Modelling and Simulation of Coking in the Riser of an Industrial Fluid Catalytic Cracking (FCC) Unit. NIJOTECH J 34(2): 301-308.

52. Missen RW, Mims CA, Saville BA (1999) Introduction to Chemical Reaction Engineering and Kinetics. John Wiley & Sons Inc., New York.

53. Fogler HS (2004) Elements of Chemical Reaction Engineering. 3rd(Edn.), Prentice Hall, New Jersey.

54. Theologos KN, Markatos NC (1993) Advanced Modeling of Fluid Catalytic Cracking Riser-Type Reactors. AIChE J 39(6): 1007-1017.

55. Martin MP, Derouin C, Turlier P, Forissier M, Wild G, et al. (1992) Catalytic Cracking in Riser Reactors: Core-Annulus and Elbow Effects. Chem Eng Sci 47(9-11): 2319-2324.

56. Kimm NK, Berruti F, Pugsley TS (1996) Modeling the Hydrodynamics of Down Flow Gas-Solids Reactors. Chem Eng Sci 51(11): 2661-2666.

57. Derouin C, Nevicato D, Forissier M, Nild G, Bernard J (1997) Hydrodynamics of Riser Units and their Impact on FCC Operation. Ind Eng Chem Res 36(11): 4504-4515.

58. Berry TA, McKeen TR, Pugsley TS, Dalai AK (2004) Two-Dimensional Reaction Engineering Model of the Riser Section of a Fluid Catalytic Cracking Unit. Ind Eng Chem Res 43(18): 5571-5581.

59. Xu O, Su H, Mu S, Chu J (2006) 7-lump kinetic model for residual oil catalytic cracking. J Zhejiang Univ Sci A 7(11): 1932-1941.

60. Sadeghbeigi R (2012) Fluid Catalytic Cracking Handbook. 3rd (Edn.), Elsevier Inc., Oxford, UK.

61. Gauthier TA (2009) Current R&D Challenges for Fluidized Bed Processes in the Refining Industry. Int J Chem Reactor Eng 7(1).

Copyright© Olafadehan OA, et al.